Model and Actuator Based Trajectory Tracking for Incremental Nonlinear Dynamic Inversion Controllers

AE5310: Thesis C&S (2021/22)

Pietro Campolucci

Delft University of Technology

TU Delft

Model and Actuator Based Trajectory Tracking for Incremental Nonlinear Dynamic Inversion Controllers

by

Pietro Campolucci

Supervisor:	Ewoud Smeur
Co-Supervisor:	Alessandro Mancinelli
Institution:	Delft University of Technology
Place:	Faculty of Aerospace Engineering, Delft
Project Duration:	09, 2021 - 08, 2022

Cover Image: ”Drone Pitturo” by Dr. Patrizio Colotto (https://www.instagram.com/pat.col8/?hl=it)

TU Delft

Contents

1

Research Paper

Model and Actuator Based Trajectory Tracking for Incremental Nonlinear Dynamic Inversion Controllers

1st Pietro Campolucci
dept. Control & Simulation
Delft University of Technology
Delft, The Netherlands
p.campolucci@student.tudelft.nl

***Abstract*—This paper proposes a control strategy based on incremental nonlinear dynamic inversion (INDI), meant for trajectory tracking purposes. The controller extends the conventional capabilities of INDI by including actuator dynamics in the inversion law and introducing a state dependent compensation term to reduce the effort of the error controller. A complementary filter is employed to reduce the degrading effect introduced by the filtering-induced delay in the feedback loop. Both simulated and real flight tests are conducted on a quadrotor configuration with artificially slowed down actuators and a drag plate mounted on top, to better observe the effect of actuator dynamics and state dependent dynamics in trajectory tracking accuracy. Simulations show that the combination of the two additional features increases tracking accuracy both in the short and long term response. It is also found that an overestimation of the state compensation term leads to instability, which makes the strategy not robust to model mismatch. Real flight tests, involving the tracking of a series of doublets on the pitch attitude and a lemniscate of Bernoulli, show that, as the complexity of the maneuver increases, the less the state compensation term effectively contributes to an improved tracking when the model is incomplete. On the other hand, trajectory tracking accuracy due to the consideration of actuator dynamics shows consistency and improvement respect to conventional INDI solutions.**

***Index Terms*—quadrotor, actuator compensation, model based compensation, trajectory tracking, incremental nonlinear dynamic inversion.**

I. Introduction

Unmanned Air Vehicles (UAVs) are becoming increasingly relevant in fast evolving industries such as inspection, surveillance and delivery [1]. While the initial use cases for UAVs asked for a limited amount of fairly simple operations, today's world demands for new applications, such as precision landing maneuvers: these are particularly critical for the correct operation of recently introduced drone-in-a-box concepts [2] or landing on moving platforms, such as a sailing ship [3]. UAVs are also required to perform precise inspections of remote infrastructures, like off-shore wind farms [4], or large ones, like railways [5]. Due to the increasing demand in automation, the demand for Unmanned Air Systems (UAS) that can take-off and land autonomously, cover large distances and be resistant to outdoor environments (strong winds, sea water etc.) is therefore increasing [6]. Such operations require both accurate trajectory tracking and long range capabilities in rough outdoor environments. To combine the two qualities, drone manufacturers often adopt a hybrid configuration [7], which uses wings-induced lift to achieve long range and endurance, and a rotorcraft configuration for precision maneuvers (e.g. landing). However, the presence of aerodynamic surfaces (e.g. wings) and slow actuators (e.g. servo-driven flaps) compromises the trajectory tracking performance of hybrid vehicles with regard to aggressive precision maneuvers [8]. As a result, the need of employing hybrid configurations for the abovementioned applications poses an interesting control problem, since accurate tracking of aggressive trajectories now needs to take into account the presence of aerodynamics surfaces and slow actuator dynamics.

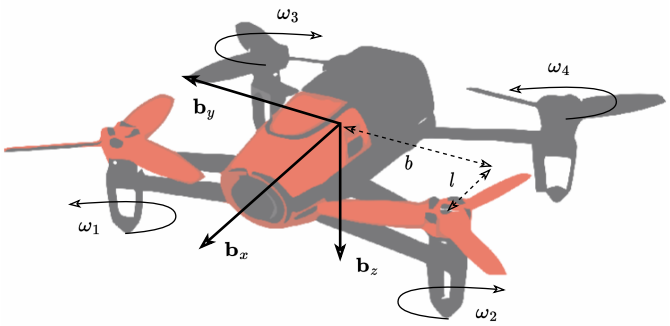

Fig. 1. Bebop I drone with overlapped body frame, moment arm and rotor directions

To achieve position and attitude control, Proportional Integral Derivative (PID) controllers are often used [9]. This strategy is usually preferred for its simplicity. However, the trajectory tracking accuracy and disturbance rejection capabilities of PID-based solutions is limited [10]. To tackle this limitation, the UAV research environment focused in the past on model based control solutions, as partial knowledge of the dynamics of a vehicle allows to tackle adaptation to its nonlinearities with a smaller effort compared to PID solutions [11]. This concept is best expressed with the nonlinear dynamic inversion (NDI) control strategy, which relies on the linearization of the

aircraft dynamics to derive the most optimal control input. Such technique proves to be effective, except in situations where the model does not match reality [12]. This turns out to be a relevant issue, as many UAVs configurations are hard to model accurately, making NDI not applicable in a wide set of scenarios.

The scientific community therefore focused in reducing model dependency by introducing the concept of incremental nonlinear dynamic inversion (INDI) [13], which increases disturbance rejection capabilities [14]. Despite the success of INDI, its robustness was so far validated in a limited set of operations, such as hover [15], as well as a limited set of vehicles, like quadrotors [16, 14] or tailsitters [17, 18]. One main limitation already addressed is the neglection of actuator dynamics in the control law [19, 20], which can lead to tracking degradation and instability when the actuators are slower than the vehicle dynamics [21]. A compensation strategy in this regard has been proposed by [19] and [22], which focused on the generation of a feedforward jerk pseudo control input in an extended INDI approach.

Another researched topic regarding conventional INDI concerns its performance towards aggressive trajectory tracking [16, 17]. In a scenario where a vehicle is programmed to track an aggressive trajectory, and it is equipped with impactful aerodynamic surfaces, the neglection of state dependent terms in the derivation of the INDI control law can lead to poor tracking performance [13]. To tackle this limitation, a differential flatness based approach was developed to allow for tracking of higher order derivatives up to snap [16], also for more complex vehicle configurations, such as tailsitters [17].

Alternatively, solutions involving the construction of model-based reference model for the generation of the pseudo control input were proposed [23, 24]. The role of reference models [25], combined with error controllers, has indeed rose interest in the research environment as it allows for the generation of smooth and feasible trajectories that can be provided to the INDI control law. In addition the two blocks can be gain tuned separately, allowing the desired system and error dynamics to be observable and configurable apart from each other. Moreover, a reference model can be introduced to a higher order. This provides a trajectory that takes into account the capabilities of the vehicle in question, such as actuator dynamics [19] or aerodynamic effects [22]. This makes the approach interesting to allow feasible and robust tracking of aggressive trajectories of a wider envelope of vehicles.

To achieve accurate tracking of aggressive trajectories in an outdoor environment, this paper proposes a control strategy, based on [21], for a quadrotor equipped with a vertically mounted drag plate and artificially slowed down actuators. The controller considers the dynamics of the actuators to generate a feedforward term of high order as pseudo control input and provides a compensation signal that takes into account the presence of additional aerodynamic surfaces. The controller is based on the mentioned incremental nonlinear dynamic inversion (INDI) control strategy, which is already known in the field for its attractive robustness to external disturbances and aerodynamic effects. Furthermore, it employs reference models and error controllers both in the inner and outer loop.

The objective of this work is to therefore enlarge the operational and vehicle envelope that can be controlled by INDI solutions, and observe its behavior is real flight tests, information that is missing in research studies conducted on the same topic [21]. The focus is mainly into observing the improvement on aggressive trajectory tracking due to the implemented augmentation on the conventional INDI structure. The strategy aims at generating a pseudo control input signal that takes into account for the vehicle dynamics. This is expected to reduce the tracking error while improving the handling of the maneuvers. For this work, a modified quadrotor is used as test platform: the actuators speed of the vehicle is severely reduced by means of an algorithm in the controller that decreases their cutoff frequency, and a drag plate is mounted on top of it (see Fig. 2), to allow aerodynamic effects to play a relevant role in the overall dynamics of the vehicle. The test platform was primarily selected for the knowledge of its model [14, 15], which allows to isolate the effect of the two modifications. The ease of implementation of the model, among with its low cost and small size, allows the platform to be tested in reality, which allows to assert the validity of the controller in a real environment, which is often subjected to model mismatch, noisy feedback signals and uncertainties.

The paper is structured as follows: firstly a description of the model of the vehicle and the drag plate are presented in Section II. A detailed structure of the controller proposed is then reported in Section III. The work then focuses on the outcome of experiments conducted both in simulation, in Section IV, and during real flights, in Section V. A conclusion is finally provided in Section VI.

II. Vehicle Model

This section formulates the dynamic model of both the Bebop I quadrotor and the drag plate mounted on top (see Fig. 2). Understanding and stating the equations that describe the motion of the UAV and the aerodynamic effects induced by the drag plate is a necessary step in order to build the actuator dynamics based controller.

A. Quadrotor Model

An isometric view of the Bebop I quadrotor is shown in Fig. 1, with its body axis, moment arms and motor spinning direction. The vectors that describe the body fixed reference frame of the vehicle are therefore $[\mathbf{b}_x\ \mathbf{b}_y\ \mathbf{b}_z]$, while for the north-east-down (NED) inertial reference frame the identity matrix $[\mathbf{i}_x\ \mathbf{i}_y\ \mathbf{i}_z]$ is used. By adopting the ZYX rotation sequence, the rotation matrix $\mathbf{R_{bi}}$ for the transformation from body to inertial reference frame is described in terms of the attitude vector $\boldsymbol{\eta} = [\phi\ \theta\ \psi]^T$ as

$$\mathbf{R_{bi}} = \begin{bmatrix} c_\theta c_\psi & -c_\phi s_\psi + s_\phi s_\theta c_\psi & s_\phi s_\psi + c_\phi s_\theta c_\psi \\ c_\theta s_\psi & c_\phi c_\psi + s_\phi s_\theta s_\psi & -s_\phi c_\psi + c_\phi s_\theta s_\psi \\ -s_\theta & s_\phi c_\theta & c_\phi c_\theta \end{bmatrix}, \quad (1)$$

where e.g. c_θ and s_θ stand for $cos(\theta)$ and $sin(\theta)$, respectively. $\boldsymbol{\eta}$ relates to the angular velocity vector in the body fixed reference frame $\boldsymbol{\Omega}$ via the matrix $\mathbf{R}_{\boldsymbol{\eta\Omega}}$ as

$$\mathbf{R}_{\boldsymbol{\eta\Omega}} = \begin{bmatrix} 1 & 0 & -s\theta \\ 0 & c\phi & s\phi c\theta \\ 0 & -s\phi & c\phi c\theta \end{bmatrix}, \tag{2}$$

The longitudinal equations of motions for the quadrotor can be written as

$$\dot{\mathbf{x}} = \mathbf{v}, \tag{3}$$
$$\dot{\mathbf{v}} = m^{-1} \cdot (\boldsymbol{F}_a(\mathbf{v}, \boldsymbol{w}) + \boldsymbol{F}_T(\boldsymbol{\eta}, T)) + g\mathbf{i}_z, \tag{4}$$

with **x** and **v** the position and velocity vectors in the inertial flame, respectively. The vector $\boldsymbol{F}_a$ indicates the aerodynamic forces acting on the vehicle, generated by the NED velocity vector **v** and the wind vector $\boldsymbol{w}$. $\boldsymbol{F}_T$ indicates the longitudinal forces originated from the collective thrust T and the vehicle attitude vector $\boldsymbol{\eta}$. Since the rotors are fixed, T is obtained by the sum of the single thrusts of all motors. Motor thrusts are dependent on the rotational speed ω_i of the propellers and the thrust coefficient k_T as

$$\boldsymbol{F}_T = \mathbf{R}_{\mathbf{bi}} \cdot \begin{bmatrix} 0 \\ 0 \\ T \end{bmatrix} = \mathbf{R}_{\mathbf{bi}} \cdot \sum_{i=1}^{4} \begin{bmatrix} 0 \\ 0 \\ -k_T \cdot \omega_i^2. \end{bmatrix} \tag{5}$$

The rotational equations of motions can be summed up in

$$\boldsymbol{\Omega} = \mathbf{R}_{\boldsymbol{\eta\Omega}} \cdot \boldsymbol{\eta}, \tag{6}$$
$$\dot{\boldsymbol{\Omega}} = \boldsymbol{J}^{-1} \cdot (-\boldsymbol{\Omega} \times \boldsymbol{J} \cdot \boldsymbol{\Omega} + \boldsymbol{M}_a + \boldsymbol{M}_T + \boldsymbol{M}_r). \tag{7}$$

The matrix $\boldsymbol{J}$ is the vehicle's inertia tensor matrix, while the last three terms represent the torques acting on the vehicle: $\boldsymbol{M}_a$ encloses the torques due to aerodynamic effects, $\boldsymbol{M}_T$ due to the different propeller thrusts and $\boldsymbol{M}_r$ due to the motor torques. The first two terms of (7) constitute the state dependent terms of the rotational dynamics, which can be grouped in the term

$$\dot{\boldsymbol{\Omega}}_x(\boldsymbol{\Omega}, \mathbf{v}) = \boldsymbol{J}^{-1} \cdot (-\boldsymbol{\Omega} \times \boldsymbol{J} \cdot \boldsymbol{\Omega} + \boldsymbol{M}_a). \tag{8}$$

$\boldsymbol{M}_T$ and $\boldsymbol{M}_r$ contribute fully to the controllable angular acceleration $\dot{\boldsymbol{\Omega}}_u$, which can be reformulated as

$$\dot{\boldsymbol{\Omega}}_u(\boldsymbol{\omega}, \dot{\boldsymbol{\omega}}) = \boldsymbol{J}^{-1} \cdot (\boldsymbol{M}_T + \boldsymbol{M}_r), \tag{9}$$

given $\boldsymbol{\omega}$ being the angular rate vector of the propellers of the quadrotor. This allows for the reformulation of (7) as

$$\dot{\boldsymbol{\Omega}} = \dot{\boldsymbol{\Omega}}_x(\boldsymbol{\Omega}, \mathbf{v}) + \dot{\boldsymbol{\Omega}}_u(\boldsymbol{\omega}, \dot{\boldsymbol{\omega}}). \tag{10}$$

Based on (5) and (9), a control vector containing both the controllable angular acceleration $\dot{\boldsymbol{\Omega}}_u$ and the collective thrust T can be obtained as

$$\begin{bmatrix} \dot{\boldsymbol{\Omega}}_u \\ T \end{bmatrix} = \frac{1}{2}\mathbf{G}_1\boldsymbol{\omega}^2 + T_s\mathbf{G}_2\dot{\boldsymbol{\omega}}, \tag{11}$$

with $\mathbf{G}_1$ being

$$\mathbf{G}_1 = 2\boldsymbol{J}_+^{-1} \begin{bmatrix} -bk_T & bk_T & bk_T & -bk_T \\ lk_T & lk_T & -lk_T & -lk_T \\ k_m & -k_m & k_m & -k_m \\ -k_T & -k_T & -k_T & -k_T \end{bmatrix} \tag{12}$$

and $\mathbf{G}_2$ being

$$\mathbf{G}_2 = T_s^{-1}\boldsymbol{J}_+^{-1} \begin{bmatrix} 0 & 0 & 0 & 0 \\ 0 & 0 & 0 & 0 \\ I_{r_{zz}} & -I_{r_{zz}} & I_{r_{zz}} & -I_{r_{zz}} \\ 0 & 0 & 0 & 0 \end{bmatrix} \tag{13}$$

with T_s being the autopilot sampling time, k_m the moment coefficient and $I_{r_{zz}}$ the rotor and propeller moment of inertia. $\boldsymbol{J}_+$ is an augmented form of the inertia tensor matrix $\boldsymbol{J}$ in order to be able to include the collective thrust equation in (11). This formulation will then be useful to derive, in the coming sections, the control laws proposed in this paper.

B. Drag Plate Aerodynamic Model

The purpose of this paper is to demonstrate how the addition of a model based state compensation term can improve the tracking of the reference trajectory for a specific type of motion. For this work, the compensation of the aerodynamic moment around the pitching axis of the quadrotor induced by a drag plate is considered.

The state compensation, for this particular case, targets only the reference produced for the control of the pitching motion, therefore the reference pitch jerk signal. As showed later in this paper, the state compensation requires modeling of the aerodynamic effects of the drag plate around the pitching axis of the quadrotor. The model is based on the plate-quadrotor configuration showed in Fig. 2: the plate is of rectangular shape with width w_p and height h_p; the center of the plate is at a distance l_p from the c.g. of the quadrotor and these two points both lie on the Y-Z plane.

If only the aerodynamic effects around the pitching axis are considered, the lift and drag coefficients of the plate, C_{l_p} and C_{d_p} respectively, are dependent on its angle of attack α with respect to the flow velocity. According to [26], for a flat plate, the aerodynamic coefficients for lift and drag vary with respect of the plate's angle of attack α as follows

$$C_{l_p} = C_{l_1} \cdot (\frac{\pi}{2} + \alpha) + C_{l_2}, \tag{14}$$
$$C_{d_p} = C_{d_1} \cdot (\frac{\pi}{2} + \alpha) + C_{d_2}, \tag{15}$$

Such coefficients, together with the resultant velocity in the earth frame V_R, can be used to obtain the resultant aerodynamic force R perpendicular to the drag plate and acting at the center of the plate

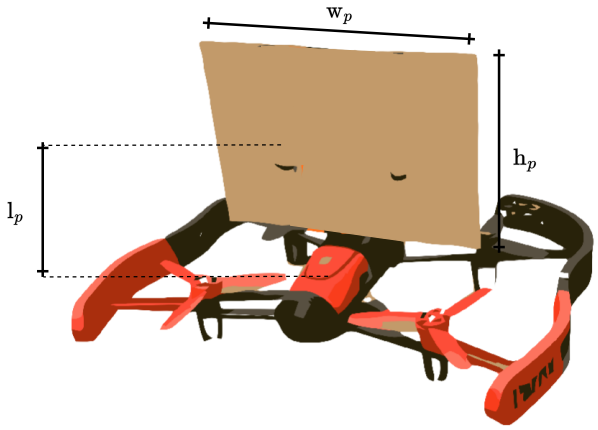

Fig. 2. Bebop I drone with drag plate mounted on top

$$D = \frac{1}{2} \cdot \rho \cdot V_R^2 \cdot w_p \cdot h_p \cdot C_{d_p}, \tag{16}$$

$$L = \frac{1}{2} \cdot \rho \cdot V_R^2 \cdot w_p \cdot h_p \cdot C_{l_p}, \tag{17}$$

$$R = (cos(\alpha) \cdot D - sin(\alpha) \cdot L) \cdot sign(V_x) \tag{18}$$

Where ρ is the air density and V_x the body velocity along the x-axis of the quadrotor. R produces an aerodynamic moment $M_{y_{dp}}$ around the body y-axis, which would then, if no other moments affect the vehicle, result in a rotational acceleration $\dot{q}_{dp}$ as follows

$$M_{y_p} = \mathrm{l}_p \cdot R, \tag{19}$$

$$\dot{q}_p = \frac{M_{y_p}}{I_{yy}}. \tag{20}$$

The acceleration generated from the drag plate is expected to deteriorate the tracking performance of the conventional INDI controller. The model of the aerodynamic forces and moments of the drag plate will be used later in the paper for the generation of the state term compensation.

III. Controller

The controller proposed in this paper consists in a cascaded, higher order INDI controller with state term compensations for rotational accelerations.

A. Cascaded INDI - Outer Loop

As previously mentioned, a cascaded INDI controller is proposed. For position control, the equation of motion for linear acceleration (4) is linearized by means of Taylor series expansion, leading to the linearized equation of motion

$$\begin{aligned}\dot{\mathbf{v}} = \dot{\mathbf{v}}_0 &\\ + \frac{\partial}{\partial \mathbf{v}} \cdot \frac{1}{m} \boldsymbol{F}_a(\mathbf{v}, \boldsymbol{w}) \mid_{\mathbf{v}=\mathbf{v}_0} (\mathbf{v} - \mathbf{v}_0) &\\ + \frac{\partial}{\partial \boldsymbol{w}} \cdot \frac{1}{m} \boldsymbol{F}_a(\mathbf{v}, \boldsymbol{w}) \mid_{\boldsymbol{w}=\boldsymbol{w}_0} (\boldsymbol{w} - \boldsymbol{w}_0) &\\ + \frac{\partial}{\partial \boldsymbol{\eta}} \cdot \frac{1}{m} \boldsymbol{F}_T(\boldsymbol{\eta}, T) \mid_{\boldsymbol{\eta}=\boldsymbol{\eta}_0} (\boldsymbol{\eta} - \boldsymbol{\eta}_0) &\\ + \frac{\partial}{\partial T} \cdot \frac{1}{m} \boldsymbol{F}_T(\boldsymbol{\eta}, T) \mid_{T=T_0} (T - T_0). &\end{aligned} \tag{21}$$

Because of the time scale separation principle [27], the second and third term in (21), which are partial to $\mathbf{v}$ and $\boldsymbol{w}$, are assumed to be negligible in magnitude respect to the fourth and fifth terms, which means that they can be removed from the equation. In addition to that, changes in yaw attitude angle ψ, part of $\boldsymbol{\eta}$, are assumed to be small [14], which allows for neglection of the term containing this partial. These assumption would then lead to

$$\begin{aligned}\dot{\mathbf{v}} &= \dot{\mathbf{v}}_0 + \mathbf{G}_o(\boldsymbol{x}_0, \boldsymbol{u}_0)(\boldsymbol{u} - \boldsymbol{u}_0) \\ &= \dot{\mathbf{v}}_0 + \mathbf{G}_o(\boldsymbol{x}_0, \boldsymbol{u}_0)\Delta\boldsymbol{u}\end{aligned} \tag{22}$$

with $\boldsymbol{u} = \begin{bmatrix}\phi & \theta & T\end{bmatrix}$ and $\mathbf{G}_o(\boldsymbol{x}_0, \boldsymbol{u}_0)$ being the summation of the non neglected terms in (21), which represents the effectiveness matrix for the outer loop controller. By rearranging the terms, the inversion law for the outer loop is obtained

$$\Delta\boldsymbol{u} = \mathbf{G}_o(\boldsymbol{x}_0, \boldsymbol{u}_0)^{-1}\boldsymbol{\nu}_o, \tag{23}$$

with

$$\boldsymbol{\nu}_o = \dot{\mathbf{v}} - \dot{\mathbf{v}}_0 \tag{24}$$

being the pseudo control input for the outer loop. $\Delta\boldsymbol{u}$ constitutes the control increment terms to be delivered to the inner loop, responsible for attitude control.

B. Rotational Jerk Tracking - Inner Loop

To build the inner loop of the cascaded INDI controller, the equation of motion expressing thrust and rotational acceleration (10) is needed. This equation is composed by controllable and state dependent terms. However, as previously mentioned, the conventional INDI structure does not take into consideration the actuator dynamics in the derivation of the inversion laws. This omission would not lead to tracking performance degradation only in the case that the actuators considered are infinitely fast, which in not the case in reality. To face this issue, [19] proposed an extension of the INDI control law in this regard. Assuming the dynamics of the motors as of first order, these can be expressed as

$$\dot{\boldsymbol{\omega}} = \mathbf{C}(\boldsymbol{\omega_{cmd}} - \boldsymbol{\omega}_0), \tag{25}$$

with $\mathbf{C}$ being a diagonal matrix containing the cutoff frequencies of the actuators and $\boldsymbol{\omega}_0$ being the actuator current state. For the Bebop, all actuators have the same cutoff

frequency, which allows for $\mathbf{C}$ to be expressed in terms of the multiplication between a scalar and a identity matrix with the size equal to the number of actuators

$$\mathbf{C} = C \cdot \boldsymbol{I}. \tag{26}$$

To fit (25) in the inversion law, (10) is differentiated, instead of undergoing linearization, leading to an expression of the rotational jerk

$$\begin{aligned}\ddot{\boldsymbol{\Omega}} = &\frac{\partial \dot{\boldsymbol{\Omega}}_x(\boldsymbol{\Omega}, \mathbf{v})}{\partial \boldsymbol{\Omega}} \cdot \dot{\boldsymbol{\Omega}} + \frac{\partial \dot{\boldsymbol{\Omega}}_x(\boldsymbol{\Omega}, \mathbf{v})}{\partial \mathbf{v}} \cdot \dot{\mathbf{v}} \\ &+ \frac{\partial \dot{\boldsymbol{\Omega}}_u(\boldsymbol{\omega}, \dot{\boldsymbol{\omega}})}{\partial \boldsymbol{\omega}} \cdot \dot{\boldsymbol{\omega}} + \frac{\partial \dot{\boldsymbol{\Omega}}_u(\boldsymbol{\omega}, \dot{\boldsymbol{\omega}})}{\partial \dot{\boldsymbol{\omega}}} \cdot \ddot{\boldsymbol{\omega}}\end{aligned} \tag{27}$$

Under the assumption of very fast actuators, the time separation principle can be applied and the first two terms in (27) can be neglected.. This allows (11) to be used with (27) to generate a set of equation of motions for the desired rotational jerk $\ddot{\boldsymbol{\Omega}}$ and thrust rate $\dot{T}$

$$\begin{bmatrix}\ddot{\boldsymbol{\Omega}} \\ \dot{T}\end{bmatrix} = \mathbf{G}_1 \boldsymbol{\omega} \dot{\boldsymbol{\omega}} + T_s \mathbf{G}_2 \ddot{\boldsymbol{\omega}}. \tag{28}$$

From (28), $\dot{\boldsymbol{\omega}}$ can be expanded from (25), while $\ddot{\boldsymbol{\omega}}$ can be expanded as

$$\begin{aligned}\ddot{\boldsymbol{\omega}} &= (\dot{\boldsymbol{\omega}} - z^{-1}\dot{\boldsymbol{\omega}}) T_s^{-1} \\ &= \mathbf{C}((\boldsymbol{\omega_{cmd}} - \boldsymbol{\omega}_0) - z^{-1}(\boldsymbol{\omega_{cmd}} - \boldsymbol{\omega}_0)) T_s^{-1}\end{aligned} \tag{29}$$

Leading to

$$\begin{bmatrix}\ddot{\boldsymbol{\Omega}} \\ \dot{T}\end{bmatrix} = \mathbf{C}(\mathbf{G}_1 \boldsymbol{\omega} + \mathbf{G}_2)(\boldsymbol{\omega_{cmd}} - \boldsymbol{\omega}_0) - \mathbf{C}\mathbf{G}_2(\boldsymbol{\omega_{cmd}} - \boldsymbol{\omega}_0) z^{-1}. \tag{30}$$

(30) can be rearranged to result in an INDI inversion law

$$\Delta\boldsymbol{\omega} = \mathbf{C}(\mathbf{G}_1 \boldsymbol{\omega} + \mathbf{G}_2)^+ \left(\begin{bmatrix}\ddot{\boldsymbol{\Omega}} \\ \dot{T}\end{bmatrix} + \mathbf{C}\mathbf{G}_2(\boldsymbol{\omega_{cmd}} - \boldsymbol{\omega}_0) z^{-1} \right), \tag{31}$$

with the operator $\circ^+$ indicating the pseudo inverse operation.

C. State Term Compensation for Pitching Motion

The extended INDI control law in (31) is meant to track the controllable rotational jerk $\ddot{\boldsymbol{\Omega}}_\mu$. In reality, state dependent rotational dynamics, such as the ones induced by aerodynamics, are present and can affect the tracking accuracy of the controller. For the case presented in this paper, the drag plate in Fig. 2 induces non negligible moments around the pitching axis, in other words, the pitch term in $\boldsymbol{M}_a$ from (7) cannot be neglected. By assuming that the moment induced by the plate its non-negligible only around the body y-axis, and other aerodynamic effects are neglected, $\boldsymbol{M}_a$ can be expressed as

$$\boldsymbol{M}_a = \begin{bmatrix}0 & M_{y_{dp}} & 0\end{bmatrix}^T, \tag{32}$$

with $M_{y_{dp}}$ from (20). For the tracking of the rotational pitch jerk, the first and second term in (27) become then non-negligible, due to the presence of high aerodynamic forces around the body y-axis. If only the aerodynamics of the drag plate are considered non-negligible, (8) can be expressed as

$$\dot{\boldsymbol{\Omega}}_x(\boldsymbol{\Omega}, \mathbf{v}) = \boldsymbol{J}^{-1}\boldsymbol{M}_a = \begin{bmatrix}0 & \frac{M_{y_{dp}}}{I_{yy}} & 0\end{bmatrix}^T \tag{33}$$

which results in a state-dependent rotational jerk component

$$\ddot{\boldsymbol{\Omega}}_x = \frac{\partial \dot{\boldsymbol{\Omega}}_x(\boldsymbol{\Omega}, \mathbf{v})}{\partial \boldsymbol{\Omega}} \cdot \dot{\boldsymbol{\Omega}} + \frac{\partial \dot{\boldsymbol{\Omega}}_x(\boldsymbol{\Omega}, \mathbf{v})}{\partial \mathbf{v}} \cdot \dot{\mathbf{v}} \tag{34}$$

that has to be included in the inversion law (31). By following the previous derivation, it is clear that the state compensation term should be subtracted from the desired rotational jerk command, leading to an inversion law that takes into consideration both the actuator dynamics and the effect of the drag plate.

$$\begin{aligned}\Delta\boldsymbol{\omega} = &\mathbf{C}(\mathbf{G}_1 \boldsymbol{\omega} + \mathbf{G}_2)^+ \\ &\left(\begin{bmatrix}\ddot{\boldsymbol{\Omega}} - \ddot{\boldsymbol{\Omega}}_x \\ \dot{T}\end{bmatrix} + \mathbf{C}\mathbf{G}_2(\boldsymbol{\omega_{cmd}} - \boldsymbol{\omega}_0) z^{-1} \right),\end{aligned} \tag{35}$$

D. Reference Model & Error Controller

The cascaded controller is meant to provide tracking of the linear acceleration error vector $\boldsymbol{\nu}_o$ from (24) in the outer loop, and the desired rotational jerk and thrust increment in the inner loop, which can be reformulated as the pseudo control input for the inner loop

$$\boldsymbol{\nu}_i = \begin{bmatrix}\ddot{\boldsymbol{\Omega}} - \ddot{\boldsymbol{\Omega}}_x \\ \dot{T}\end{bmatrix} \tag{36}$$

Both terms, $\boldsymbol{\nu}_o$ and $\boldsymbol{\nu}_i$ are higher order derivatives of the commanded signal to the loops. Based on sensor feedback and desired dynamics, these terms can be obtained by means of a combination of a reference model (RM) with an error controller (EC). Given the state vector command

$$\boldsymbol{\sigma} = \begin{bmatrix}\mathbf{x} & \psi\end{bmatrix}_{cmd} \tag{37}$$

a set of gains $\boldsymbol{K}_o$, which indicates the desired longitudinal dynamics of the vehicle, is used in an outer loop RM to obtain the reference longitudinal acceleration $\dot{\mathbf{v}}_{ref}$ and the external reference trajectory

$$\boldsymbol{\xi}_o = \begin{bmatrix}\mathbf{v} \\ \mathbf{x}\end{bmatrix}_{ref}. \tag{38}$$

For disturbance rejection, an outer loop EC is set with gains $\boldsymbol{K}_{oE}$ that describe the error dynamics. The EC considers the error between $\boldsymbol{\xi}_o$ and the sensor based signals $\mathbf{v}_0$ and $\mathbf{x}_0$ to provide an error compensation signal $\dot{\mathbf{v}}_{ec}$, which contributes to the generation of the pseudo control input

$$\boldsymbol{\nu}_o = \dot{\mathbf{v}}_{ref} + \dot{\mathbf{v}}_{ec} - \dot{\mathbf{v}}_0 \tag{39}$$

In a similar fashion, the commanded attitude vector, obtained partly from the outer loop output (θ_{cmd} and ϕ_{cmd}) and partly from $\boldsymbol{\sigma}$ (ψ_{cmd}), is used for the generation of the desired rotational jerk signal that composes $\boldsymbol{\nu}_i$, with the thrust rate $\dot{T}_{ref}$ straightforwardly obtained from the outer loop output. To do that, a 3rd order reference model is constructed in the inner loop for the generation of the reference rotational jerk signal $\ddot{\boldsymbol{\Omega}}_{ref}$, by means of a set of desired gains $\boldsymbol{K}_i$ that generate feasible and optimal rotation dynamics. To achieve optimality, the gains used for rotational jerk dynamics have the same magnitude of the common cutoff frequency C of the actuators. The lower order reference trajectory vector

$$\boldsymbol{\xi}_i = \begin{bmatrix} \dot{\boldsymbol{\Omega}} \\ \boldsymbol{\Omega} \\ \boldsymbol{\eta} \end{bmatrix}_{ref} \tag{40}$$

is used together with the sensor based feedback signals in the inner error controller. A set of gains $\boldsymbol{K}_{iE}$ are used together with C to generate the jerk compensation signal $\ddot{\boldsymbol{\Omega}}_{ec}$, as proposed by [21]. This leads to a reformulation of the pseudo control input as

$$\boldsymbol{\nu}_i = \begin{bmatrix} \ddot{\boldsymbol{\Omega}}_{ref} + \ddot{\boldsymbol{\Omega}}_{ec} - \ddot{\boldsymbol{\Omega}}_x \\ \dot{T}_{des} \end{bmatrix} = \begin{bmatrix} \ddot{\boldsymbol{\Omega}} \\ \dot{T} \end{bmatrix}_{des} \tag{41}$$

E. Complementary Filter

In reality, the gyroscope delivers the measured signal in addition with noise. To avoid the noise to propagate through the controller, filters can be used. Such signals have been filtered in cascaded INDI controllers by equally filtering the noisy rotational acceleration signal and the actuator feedback to the control increment, to have them in phase [15].

While the controllable rotational jerk $\ddot{\boldsymbol{\Omega}}_\mu$ can still be synchronized with the actuators feedback, the state compensation term $\ddot{\boldsymbol{\Omega}}_x$ cannot. The inability to provide a global synchronization can severely deteriorate the improvement of the proposed controller over conventional solutions.

For this reason a filter that can remove noise and remove the existing delay must be implemented. [20] proposes the use of a 2nd order complementary filter based on a model based estimation of the angular acceleration and the real measurement. As shown in Fig. 3, the estimated signal $\dot{\boldsymbol{\Omega}}_{\mathbf{P}}$ is filtered with the same filter $\boldsymbol{H}(z)$ used for the measured signal $\dot{\boldsymbol{\Omega}}$; the delay induced by the filtering obtained from the model is then used to compensated for the induced delay on the main signal, which provides an undelayed, filtered estimation for the rotational acceleration $\hat{\dot{\boldsymbol{\Omega}}}$. The generation of the estimated signal $\dot{\boldsymbol{\Omega}}_{\mathbf{P}}$ requires a good understanding of the control effectiveness of the vehicle, which is employed also in the INDI control law, and state dependent terms. Since a quadrotor is considered, the only state dependent term that is believed to deliver a non negligible impact to the estimation of the angular acceleration, is the drag plate. For this reason, $\dot{\boldsymbol{\Omega}}_{\mathbf{P}}$ can be decomposed further in

$$\dot{\boldsymbol{\Omega}}_{\mathbf{P}} = \dot{\boldsymbol{\Omega}}_{\mathbf{G}} + \dot{\boldsymbol{\Omega}}_{\mathbf{A}}. \tag{42}$$

As also shown in Fig. 3, $\dot{\boldsymbol{\Omega}}_{\mathbf{G}}$ indicates the estimation of the angular acceleration induced by the actuators, while $\dot{\boldsymbol{\Omega}}_{\mathbf{A}}$ the one induced by aerodynamic effects; for this work, the only aerodynamic effect considered is the one of the drag plate. $\dot{\boldsymbol{\Omega}}_{\mathbf{A}}$ requires then an accurate estimation of the aforementioned. This nomenclature will also be used in the presentation of the experimental results. With the same method, an undelayed estimation for the linear acceleration $\hat{\dot{\mathbf{v}}}$ can also be obtained.

F. Full Controller Overview

The subsections above describe the components of the full, cascaded INDI controller, augmented with actuator dynamics compensation and a state term compensator for the drag plate mounted on top. The controller can be divided mostly in three parts: the outer loop for position control, the inner loop for attitude control and the complementary filter. The first can be viewed schematically in the block diagram from Fig. 4, while the last two can be viewed in Fig. 5. For an even better understanding of the roles of each component of the controller and the structure of the pipeline, Table I is available. The coming section compares the proposed solution with other configurations.

IV. Simulation Results

The proposed controller is meant to provide the capabilities to accurately track trajectories even when the vehicle presents properties that severely degrade the performance of conventional INDI controllers, such as slow actuators or wide aerodynamic surfaces. For this analysis, a simulation of the proposed vehicle, a Parrot Bebop I quadrotor equipped with drag plate and slow actuators, is considered. Since the effect of the plate is such that its biggest disturbance contribution is on the pitch axis, this analysis will look at the response of the controller to a negative pitch angle step response. Due to the step requested in a negative direction, the vehicle is expected to progressively gain a forward velocity, which increasingly affects the aerodynamic moment exerted on the vehicle. This setup would then allow to fully observe and assess the behavior of the controller towards these particular dynamics. The effect of this controller can be the verified in real world flight tests in Section V.

A. Tracking Accuracy

The main indicator of performance of the proposed controller is how much better it can track the reference trajectory. This is provided by the reference model, and to assess the tracking accuracy of the different configurations, the desired dynamics of the RM must be the same for all. For this analysis, a 3rd order reference model is adopted with the gains in Table II.

The tracking accuracy is compared between a conventional INDI controller, an extended version with actuator compensation (ACINDI) and the proposed controller, which includes the state compensation term for the drag plate (ASCINDI). The performance of each can be observed visually in Fig. 6. In the short interval of time that follows the initiation of the

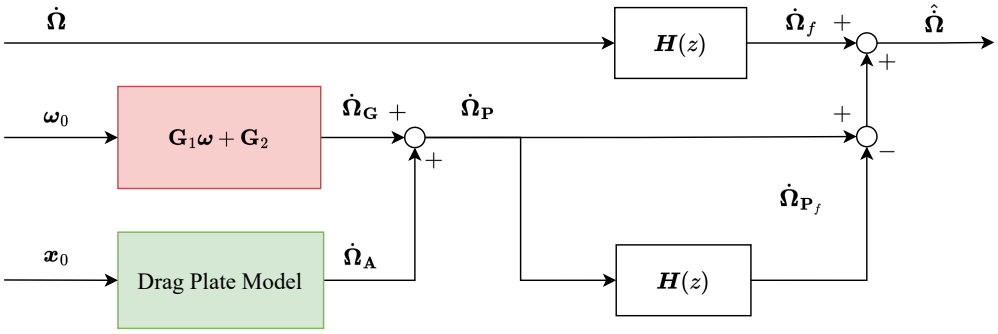

Fig. 3. Complementary filter scheme for the processing of the angular acceleration $\dot{\boldsymbol{\Omega}}$

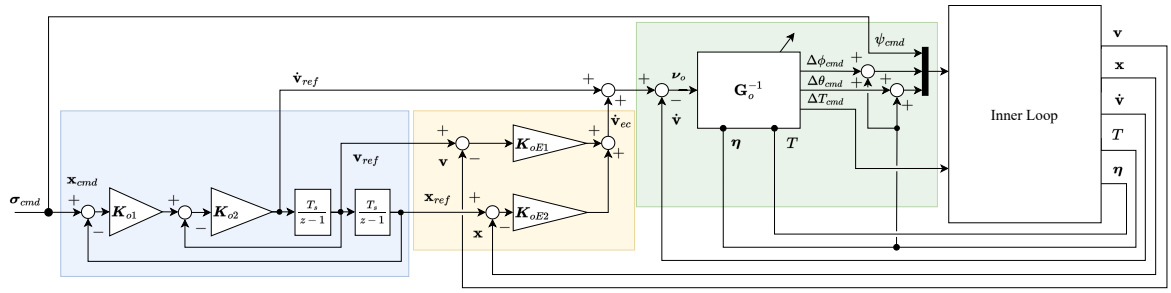

Fig. 4. Outer loop of full controller, composed by: reference model (blue), error controller (yellow), inversion law for attitude and thrust increment commands (green)

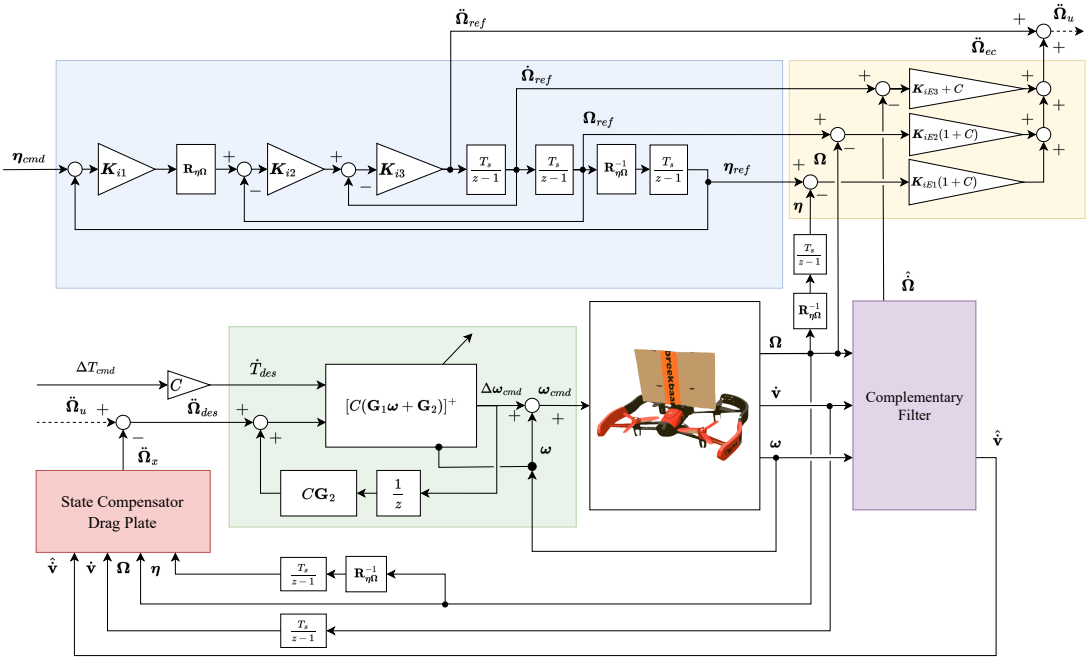

Fig. 5. Inner loop of full controller, composed by: reference model (blue), error controller (yellow), state compensation term (red), inversion law for actuator command generation (green), complementary filter (purple)

command (at sec 2, first vertical dotted line), the drag plate is not subjected to enough velocity to deteriorate the performance of the controllers, but it is clear that the consideration of actuator dynamics is important for the short term response. By omitting the "speed" capability of the actuators, the INDI controller immediately lags behind the reference, causing the

TABLE I
CONTROLLER PIPELINE

Block Name	Role	Input	Output
Outer Loop RM	Reference trajectory for OL	$\boldsymbol{\sigma}_{cmd}$	$\dot{\mathbf{v}}_{ref}$, $\boldsymbol{\xi}_o$
Outer Loop EC	Error compensation for OL	$\boldsymbol{\xi}_o$, $\mathbf{v}$, $\mathbf{x}$	$\dot{\mathbf{v}}_{ec}$
Outer Loop INDI	Inversion Law for OL	$\dot{\mathbf{v}}_{des}$, $\hat{\dot{\mathbf{v}}}$	$\boldsymbol{\eta}_{cmd}$, ΔT_{cmd}
Inner Loop RM	Reference trajectory for IL	$\boldsymbol{\eta}_{cmd}$	$\ddot{\boldsymbol{\Omega}}_{ref}$, $\boldsymbol{\xi}_i$
Inner Loop EC	Error compensation for IL	$\boldsymbol{\xi}_i$, $\hat{\boldsymbol{\Omega}}$, $\dot{\boldsymbol{\Omega}}$, $\boldsymbol{\eta}$	$\ddot{\boldsymbol{\Omega}}_{ec}$
State Compensator Drag Plate	Model based drag plate effect compensation	$\hat{\dot{\mathbf{v}}}$, $\dot{\mathbf{v}}$, $\dot{\boldsymbol{\Omega}}$, $\boldsymbol{\eta}$	$\ddot{\boldsymbol{\Omega}}_x$
Inner Loop INDI	Inversion law for inner loop	$\ddot{\boldsymbol{\Omega}}_{des}$, $\boldsymbol{\omega}$, ΔT_{cmd}	$\boldsymbol{\omega}_{cmd}$
Complementary filter	Model based filtering of noisy states	$\boldsymbol{\omega}$, $\dot{\boldsymbol{\Omega}}$, $\dot{\mathbf{v}}$	$\hat{\dot{\mathbf{v}}}$, $\hat{\dot{\boldsymbol{\Omega}}}$

TABLE II
RM AND EC GAINS USED FOR THE RESPONSE ANALYSIS

Gain	Value
$\boldsymbol{K}_{\boldsymbol{\eta}}$	diag([7, 7, 7])
$\boldsymbol{K}_{\boldsymbol{\Omega}}$	diag([15, 15, 15])
$\boldsymbol{K}_{\dot{\boldsymbol{\Omega}}}$	diag([20, 20, 20])
$\boldsymbol{K}_{\boldsymbol{\eta E}}$	diag([50, 50, 50])
$\boldsymbol{K}_{\dot{\boldsymbol{\Omega}} \boldsymbol{E}}$	diag([13, 13, 13])
$\boldsymbol{K}_{\boldsymbol{\eta E}}$	diag([9, 9, 9])

first peak in error (blue line in Fig. 6). Contrarily, the ACINDI and ASCINDI solutions provide an immediate accurate response to the step, performing equally well. The jerk tracking method therefore results valid to achieve an accurate short term response to commanded trajectories. Shortly after the initial response however (second dotted line at 3 seconds), the aerodynamic moment exerted on the drag plate causes the first two controllers to produce an increasing tracking error due to the increase in velocity, for which the sole error controller is not able to effectively correct for. This is not the same for the proposed controller, which considers the presence of the drag plate in the generation of the pseudo control input.

B. Robustness to Model Mismatch

A serious limitation to real world applications which applies to model based controllers is the presence of inaccuracies in the estimation of the model. An inaccurate understanding of the model can compromise the benefit of including it in the first place, or even leading to instability. Here, the robustness of the ASCINDI controller is discussed. The term in the controller's architecture that mostly relies on the accuracy of the model is the state compensation term $\ddot{\Omega}_x$, which computes the rotational jerk component of the drag plate and affects directly the pseudo control input delivered to the inversion law. It is important to understand how the response would change for two cases: when $\ddot{\Omega}_x$ overestimates the influence of the drag plate, so it acts more aggressively than necessary, and when it underestimates it, so it considers its effects less relevant. By looking at Fig. 7, the effect of both can be observed. By progressively scaling the perfect matching compensation signal in an interval from 0 (no compensation) to 2 (the effect

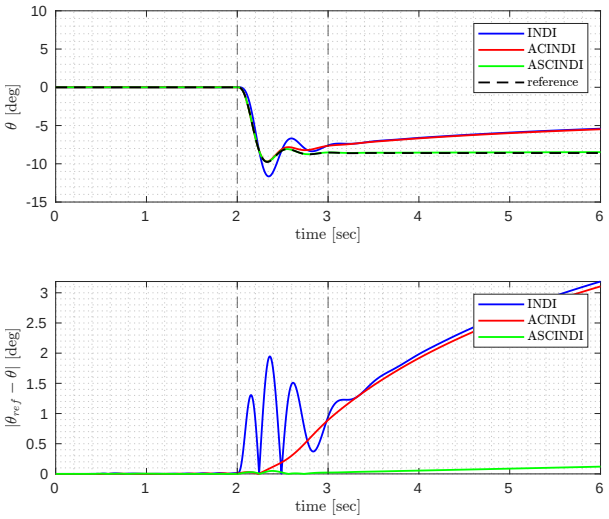

Fig. 6. Tracking response of discussed controllers: matching of reference trajectory (above), absolute error between response and reference trajectory (below)

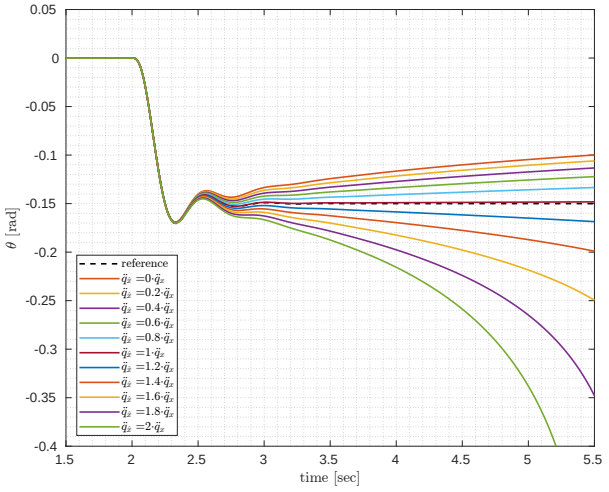

Fig. 7. Effect of model mismatch on the reference tracking performance of the ASCINDI controller

of the drag plate is twice as strong as in reality), a conclusion can be made on the two mentioned cases. By increasingly underestimating the effect of the plate, the response will converge to the response provided by a ACINDI controller. On the other hand, an overestimation of the drag plate effect can seriously compromise the stability of the platform. For all the overestimated responses in Fig. 7, the state compensator term leads to instability. This is because the error controller is not able to compensate for this signal with the increase in velocity, which asks for a more aggressive compensation. In the light of this, once real flight tests are performed, it is important not to overestimate the effect of the aerodynamic effects, but rather be conservative, as an underestimation still leads to a tracking improvement with respect to an ACINDI controller.

C. Complementary Filter Effect

It was previously mentioned how the effect of delay induced by filtering of noisy signals, such as accelerations, has a significant degrading effect on the performance of the controller. The increased complexity (i.e. introduction of drag plate model in the feedback to the increment) required to perform phase synchronization in the proposed controller makes the removal of the delay the only solution. This removal can be achieved by the addition of a complementary filter, which relies on an accurate estimation of the vehicle dynamics. As for the state compensation term, the complementary filter performance is also dependent on the accuracy of the model. However, the filter only uses the difference between the estimated signal and its filtered version to estimate the undelayed signal to feed to the controller. This means that, given model inaccuracies in the complementary filter, these should mostly affect the tracking only in case of large changes in acceleration. This is clear by looking at Fig. 8: similarly to Fig. 7, the estimated angular acceleration around the body Y-axis $\dot{q}_{\mathbf{P}}$ in the complementary filter is scaled by a factor varying from 0 (no delay removal) to 2 (the delay removal is based on an acceleration estimation that is twice in magnitude respect to the measured acceleration). In the case where no delay estimation is provided (scaling factor of 0), the phase becomes too large for most filters leading to an unstable oscillation. This enforces the importance of delay consideration and the effectiveness of the complementary filter.

V. Experimental Results

This chapter illustrates the validation process conducted around the proposed controller. For this, both simulated and real flight tests have been conducted on a modified version of the Bebop I quadrotor. For the real flights, both a series of step inputs to the pitch attitude and a lemniscate trajectory of Bernoulli are involved. These maneuvers are involved in the drag plate model optimization and in the application of the state compensation term, separately. The setup and nature of the tests, among with their outcome, is presented here.

A. Setup

To test the proposed INDI control, the Parrot Bebop I drone shown in Fig. 1 is used. As already mentioned, the proposed

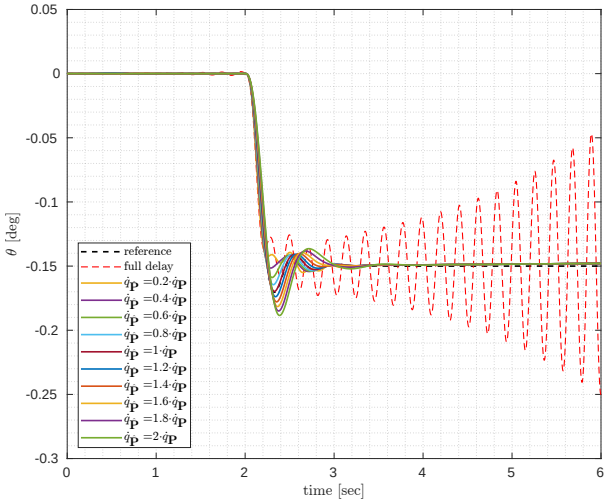

Fig. 8. Effect of model mismatch in the complementary filter on the reference tracking performance of the ASCINDI controller

controller is expected to be effective in particular scenarios where the platform is equipped with wide aerodynamic surfaces and/or actuators slower then the body dynamics of the platform. The conventional settings of the considered drone do not fit in this category, but the platform was selected for its simple model and extensive documentation on its autopilot. To make the Bebop I fit in the interested configuration, two modifications were applied to the vehicle. Firstly a 23 cm by 16 cm drag plate, shown in Fig. 2 was mounted on the top of the vehicle at 12 cm from the position of its c.g., with its normal vector pointing in the direction of the body x-axis. Secondly, the cutoff frequency of the actuator dynamics was artificially reduced through the use of a digital lag filter. It was therefore possible to decrease the speed of the actuators from the nominal value of 50 rad/sec to 20 rad/sec. For filtering of accelerations, a 2nd order Butterworth lowpass filter is employed both in the INDI configuration and in the complementary filters used in the extended controllers, with a cutoff frequency of 5 rad/sec. The vehicle runs on Paparazzi Autopilot firmware at 512 Hz.

B. Drag Plate Model Parameters Optimisation

The state term compensation signal for the drag plate, as mentioned previously, is heavily dependent on its model. Both the complementary filter and the state jerk compensation signal rely then on its accuracy. Assuming that the model derived is correct for the effect of the drag plate on the pitching axis is mathematically representative of the physics involved, there is still no knowledge of the real magnitude of the coefficients that affect lift and drag estimation of the plate in (15) and (14). Based on existing research on flat plate aerodynamics [26], an initial guess can be provided to the model, but more extensive fine tuning of such parameters is required for better model matching. For this work, only the aerodynamic moment of the drag plate induced around the body Y-axis is considered in the optimization and the controller. The following optimization

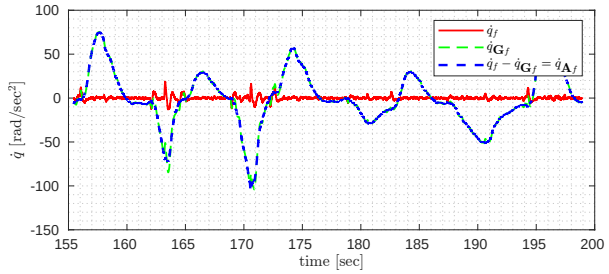

Fig. 9. Effect of drag plate on perceived rotational acceleration based on actuator state, for a series of doublets

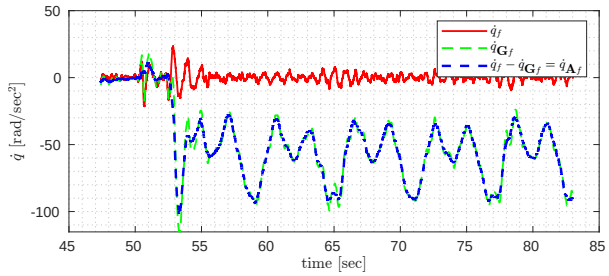

Fig. 10. Effect of drag plate on perceived rotational acceleration based on actuator state, for a lemniscate trajectory

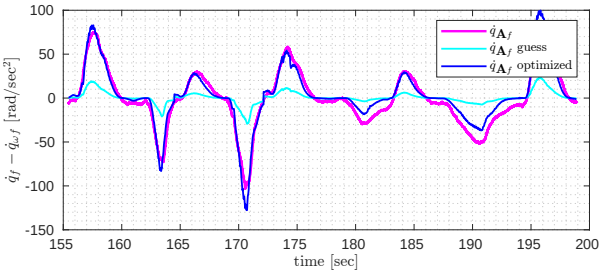

Fig. 11. Effect of drag plate on perceived rotational acceleration based on actuator state

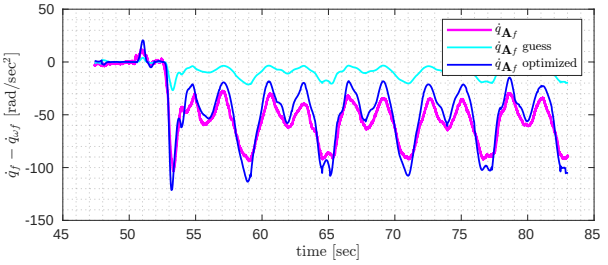

Fig. 12. Effect of drag plate on perceived rotational acceleration based on actuator state

regards then only the pitch acceleration $\dot{q}$, instead of the whole rotational acceleration vector $\dot{\mathbf{\Omega}}$. By referring to the nomenclature in Section III-E, parameter optimisation is performed by comparing the filtered rotational pitch acceleration of the vehicle $\dot{q}_f$, estimated from the gyroscope output, with the one estimated by a complementary filter lacking the drag plate model $\dot{q}_{\mathbf{G}f}$, filtered. Without the drag plate, and neglecting additional aerodynamic effects, $\dot{q}_f$ and $\dot{q}_{\mathbf{G}f}$ should match. However, because the drag plate is mounted on the vehicle, the drag plate induced rotational pitch acceleration $\dot{q}_{\mathbf{A}f}$ plays a non negligible role. As explained in Section III-E, $\dot{q}_{\mathbf{A}f}$ can be observed during flight tests by looking at the difference between the measured acceleration and the one estimated by the actuators only

$$\dot{q}_{\mathbf{A}f} = \dot{q}_f - \dot{q}_{\mathbf{G}f}. \tag{43}$$

To assert this, two different flight tests were conducted: a series of doublets on the pitch attitude and a lemniscate of Bernoulli, shown visually in Fig. 17. The relevance of $\dot{q}_{\mathbf{A}f}$ can be clearly seen in both in Fig. 9, for the doublets, and Fig. 10, for the lemniscate. Due to the velocity increase, the aerodynamic moment induced by the plate increases, worsening the mismatch.

[26] provides an empirical set of aerodynamic coefficients for the drag plate model presented in (14) and (15). However, such coefficients can be further tuned to fit the effect of the drag plate recorded during real flight tests. In order to tune the aerodynamic coefficients to fit the real flight observations, a Trust Region Reflective (TRF) algorithm is employed for the optimization. The TRF is provided with upper and lower bounds for each coefficients, as indicated in Table III.

TABLE III
AERODYNCAMIC COEFFICIENTS UPPER AND LOWER BOUNDS

-	C_{d_1}	C_{d_2}	C_{l_1}	C_{l_2}
b_u	5	2	0	3
b_l	0	0.6	-5	1.5

By running the TRF optimization on both flight tests, a factor 10 decrease in MSE between the real $\dot{q}_{\mathbf{A}f}$ and the estimated one is achieved, as indicated in Table IV. The result of the optimization for $\dot{q}_{\mathbf{A}f}$ can also be seen in Fig. 11, for the doublet test, and in Fig. 12, for the lemniscate.

TABLE IV
MSE REDUCTION IN DRAG PLATE INDUCED ROTATIONAL ACCELERATION DUE TO OPTIMIZATION BY MEANS OF TRF ALGORITHM (MSE IN [RAD^2/SEC^4])

Coefficients $[C_{d_1}, C_{d_2}, C_{l_1}, C_{l_2}]$	**MSE Step**	**MSE Lemniscate**
[0.0033, 0.7, -0.0228, 2.01]	689.32	1850.61
[0.0035, 2, -0.000249, 3]	64.27	173.17

By looking at the MSE for both tests and the corresponding figures, it can be seen that the model provides a better fit for the doublet series test compared to the lemniscate. This is because the former excites mostly the pitch motion, while the latter includes also the other two motions that the model proposed here does not take into account. The decrease in fitting performance for the lemniscate can be also seen by looking at Fig. 13 and Fig. 14. Because of the limits of the

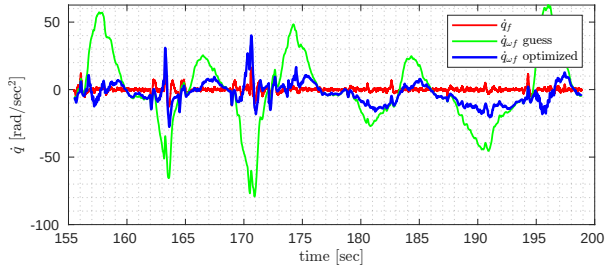

Fig. 13. Effect of drag plate on perceived rotational acceleration based on actuator state

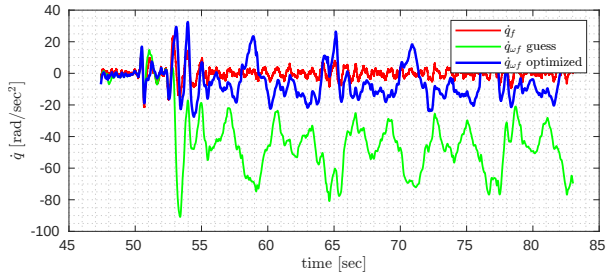

Fig. 14. Effect of drag plate on perceived rotational acceleration based on actuator state

model in a more complicated maneuver, a decrease in tracking accuracy due to model mismatch can be expected for the lemniscate, as shown in the following sections.

C. Step Impulse Tracking

The first results presented in this paper concern the tracking performance of a step input in the pitch attitude angle, as in the simulation results presented in Section IV. The controllers subjected to this test are listed in Table V.

TABLE V
CONTROLLER CONFIGURATIONS SELECTED FOR TESTING

Controller	**Additions**
INDI	None
ACINDI	Jerk Tracking through Actuator Compensation and Complementary Filters Enabled
ASCINDI	Jerk Tracking through Actuator Compensation, State Term Compensation and Complementary Filters Enabled

All controllers were subjected to a consecutive series of pitch attitude steps of -0.15 radians for 3 seconds. The total number of steps per controller was 5. All inversion laws were provided with a similar set of gains which allowed for fair comparison between the tracking performance of the different controllers. Fig. 15 shows the tracking performance of the considered controller configurations of one of the series of steps. It can immediately be seen that the effect of the drag plate does not allow the conventional INDI solution to reach the attitude setpoint during the whole duration of the step, while the two extended configurations do. Both the ACINDI and the ASCINDI configuration have a drag plate model in the complementary filter, which further helps convergence to the setpoint, but the state compensation term effect (magenta line) allows for a faster convergence to the setpoint compared to the ACINDI configuration. However, the ASCINDI controller does not manage to keep the reached setpoint for the whole duration of the step, but instead oscillates around it undesirably. This is caused by a possible overestimation of the model used for the state compensation term generation that results in the controller to overshoot the setpoint. In addition, both extended solutions fail to track the short term trajectory effectively. Again, it can be dependent by the model proposed, which does not take into account rotational moments induced by the rotational acceleration of the vehicle, but only by its longitudinal motion. Overall, the calculated RMSE over all steps between the attitude reference and the actual state amounts to 0.0126 deg for the INDI configuration, while it decreases to 0.0070 for the ACINDI controller and 0.0067 for the ASCINDI controller. It is therefore clear that while the actuator compensation and the complementary filter significantly benefit the performance of the controller with respect to a conventional structure, the state compensation term based on a model with optimized parameters does not greatly impact the trajectory tracking performance.

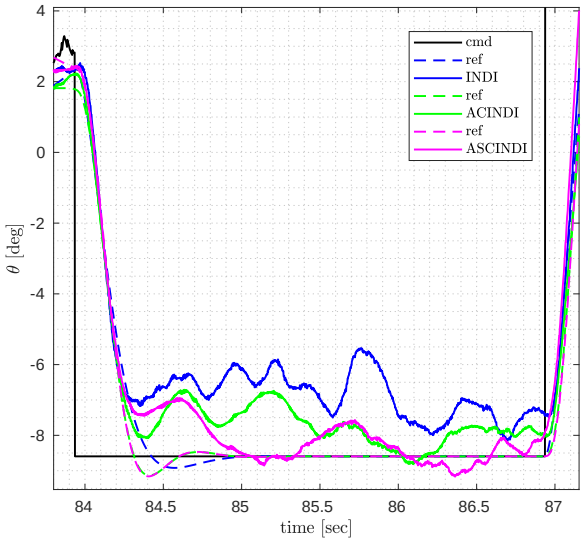

Fig. 15. Trajectory tracking performance of step input reference of different controllers

D. Lemniscate Trajectory Tracking

To provide a more broad overview of the controllers quality, the tracking performance of a Lemniscate of Bernoulli is provided. Each controller is tested on 3 laps of a 3.2x1.6 meters trajectory followed in a lap time of 12 seconds per lap. During this maneuver, the vehicle reaches a top speed of 2.81 m/sec. The controller configurations tested are the same as for the doublet tracking, as mentioned in Table

V. The performance in terms of position and velocity can be seen in Fig. 17. Visually, it can be seen that the state compensation term negatively affects the velocity tracking performance, as it is subjected to oscillations non visible in the other two controllers. This is indicated in Table VI, where for overall position tracking the ACINDI configuration scores best overall, with the ASCINDI controller performing worse than the conventional INDI solution.

TABLE VI
RMSE BETWEEN REFERENCE AND STATE FOR POSITION AND ATTITUDE DURING LEMNISCATE TRAJECTORY TRACKING

RMSE	INDI	ACINDI	ASCINDI
x	0.071522	0.048414	0.087904
y	0.068977	0.073452	0.073649
z	0.064526	0.041485	0.096018
ϕ	0.038409	0.035212	0.047385
θ	0.054953	0.026039	0.054015
ψ	0.022945	0.013425	0.020134

A best assessment on the proposed controller can be done by looking at the performance in attitude tracking. Fig. 17 shows the overall attitude trajectory together with the absolute error between the reference and the state. As suggested by the position tracking, the ACINDI solution achieves an overall tracking error in attitude that is lower than INDI and ASCINDI. Table VI also shows that, despite the pitch attitude is the most perturbed by the effect of the drag plate, ACINDI provides the highest improvement in tracking respect to INDI exactly for the pitch attitude. As mentioned previously, the ACINDI configuration employs a complementary filter with a drag plate model. Despite the asserted model incompleteness, it seems that the ACINDI controller benefits from the presence of the drag plate model in the complementary filter. This is in line with what was presented in Section IV-C regarding the robustness of the complementary filter to model mismatch.

On the other hand, based on the findings about the robustness of the state compensation term to model mismatch, reported in Fig. 7, and based on the asserted incompleteness of the model for the application on complex trajectories, such as the lemniscate, it could be claimed that the state compensation term for this flight is overestimating the real drag plate model. As previously discussed, an overestimation the drag plate model can lead to instability, which is the case for the test conducted. In order to assert this hypothesis, multiple lemniscate flight tests have been conducted, by gradually down-scaling the state compensation term up to a point where the controller acts as a ACINDI configuration (i.e. no state compensation term). By looking at the RMSE between the reference pitch attitude and the measured attitude, an gradual improvement in RMSE can be detected by scaling down the term. As visible from Fig. 16, a minimum is reached before reaching the full cancellation of the term (at 0.2 times the initially provided model). This indicates that the provided model, despite optimization, greatly overestimates the effect of the plate, leading to a large deviation.

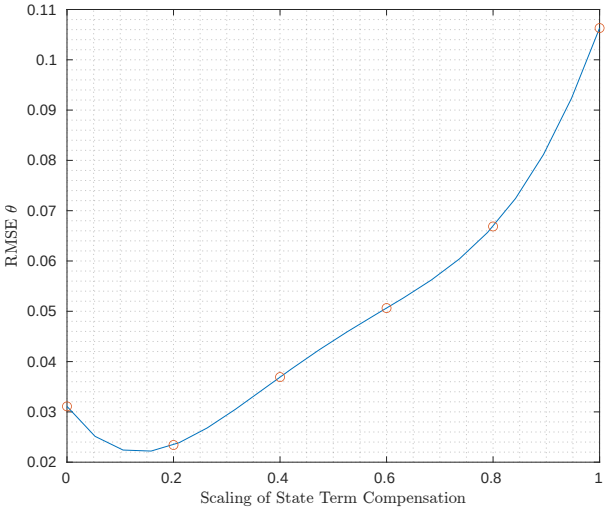

Fig. 16. Decrease in RMSE in tracking of pitch attitude reference due to down-scaling of the state compensation term, from 1 (full term) to 0 (no term)

The required model complexity for such maneuver cannot be met by considering only the pitching moment, as opposed to the doublet flight test, reason why the state compensation term is less reliable.

VI. CONCLUSIONS

This paper proposed a novel control strategy based on INDI that is meant to provide an improvement in trajectory tracking for vehicles with slow actuators and strong aerodynamic effects. The controller takes into consideration the dynamics of the actuators of the vehicle by tracking the desired rotational jerk signal, instead of acceleration. The presence of a drag plate mounted on top of the vehicle is also modeled and employed by the complementary filter used for acceleration noise reduction and by the state compensation term, which aims to modify the feedforward pseudo control input in the inner loop to counteract the disturbing effects of the plate. Through response analysis, it was found that an overestimation of the effects of the drag plate in the generation of the state compensation can lead quickly to instability. On the other hand, the presence of the drag plate model in the complementary filter results to be beneficial to the overall tracking despite the presence of model inaccuracies. This was further validated in real flight tests. From simple step maneuvers and a more complex lemniscate trajectory, it turns out that the state compensation contribution is limited to detrimental, due to the low robustness to model mismatch. On the other hand, substantial improvements compared to conventional INDI were obtained for the controller configuration which included actuator compensation and complementary filter. During lemniscate trajectory, the tracking error for the

pitch attitude is reduced by more than 50%. This happened despite the pitch being the state that is mostly disturbed by the presence of the drag plate. This suggests that the presence of the model of drag plate in the complementary filter has a beneficial impact in trajectory tracking, and, on the contrary of the state compensation term, is robust to model inaccuracies.

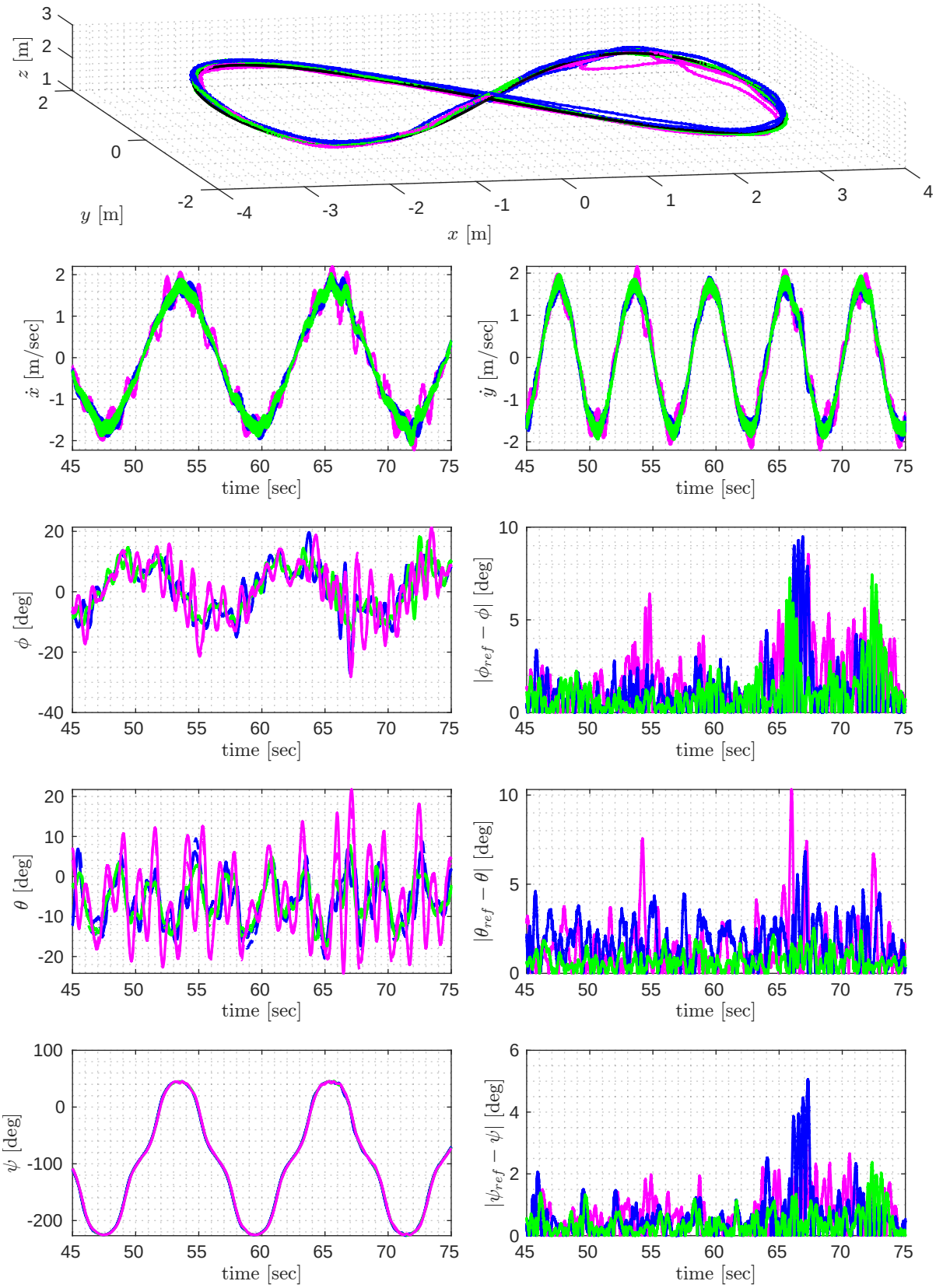

Fig. 17. Overview of position, velocity and attitude tracking of the lemniscate trajectory for the three proposed controllers: INDI (blue), ACINDI (green), ASCINDI (magenta)

References

[1] Omid Maghazei, Michael A Lewis, and Torbjørn H Netland. "Emerging technologies and the use case: A multi-year study of drone adoption". In: *Journal of Operations Management* n/a.n/a (June 2022). ISSN: 0272-6963. DOI: https://doi.org/10.1002/joom.1196. URL: https://doi.org/10.1002/joom.1196.

[2] Helge-André Langåker et al. "An autonomous drone-based system for inspection of electrical substations". In: *International Journal of Advanced Robotic Systems* 18.2 (Mar. 2021), p. 17298814211002973. ISSN: 1729-8806. DOI: 10.1177/17298814211002973. URL: https://doi.org/10.1177/17298814211002973.

[3] C De Wagter et al. "The NederDrone: A hybrid lift, hybrid energy hydrogen UAV". In: *International Journal of Hydrogen Energy* 46.29 (2021), pp. 16003–16018. ISSN: 0360-3199. DOI: https://doi.org/10.1016/j.ijhydene.2021.02.053. URL: https://www.sciencedirect.com/science/article/pii/S0360319921005371.

[4] Hwei-Ming Chung et al. "Placement and Routing Optimization for Automated Inspection with UAVs: A Study in Offshore Wind Farm". In: *IEEE Transactions on Industrial Informatics* 17 (June 2021), pp. 3032–3043. DOI: 10.1109/TII.2020.3004816.

[5] Koppány Máthé and Lucian Busoniu. "Vision and Control for UAVs: A Survey of General Methods andof Inexpensive Platforms for Infrastructure Inspection". In: *Sensors (Basel, Switzerland)* 15 (June 2015), pp. 14887–14916. DOI: 10.3390/s150714887.

[6] Ferran Giones and Alexander Brem. "From toys to tools: the co-evolution of technological and entrepreneurial developments in the drone industry". In: *Business Horizons* 60.6 (2017), pp. 875–884. ISSN: 0007-6813. DOI: 10.1016/j.bushor.2017.08.001.

[7] Adnan S Saeed et al. "A survey of hybrid Unmanned Aerial Vehicles". In: *Progress in Aerospace Sciences* 98 (2018), pp. 91–105.

[8] Nihal Dalwadi, Dipankar Deb, and Jagat Jyoti Rath. "Biplane Trajectory Tracking Using Hybrid Controller Based on Backstepping and Integral Terminal Sliding Mode Control". In: *Drones* 6.3 (Feb. 2022), p. 58. ISSN: 2504-446X. DOI: 10.3390/drones6030058. URL: https://www.mdpi.com/2504-446X/6/3/58.

[9] Chao Chen et al. "Control and flight test of a tilt-rotor unmanned aerial vehicle". In: *International Journal of Advanced Robotic Systems* 14 (Feb. 2017), p. 172988141667814. DOI: 10.1177/1729881416678141. URL: 10.1177/1729881416678141.

[10] Ronald van 't Veld, Erik-Jan Van Kampen, and Q Ping Chu. "Stability and Robustness Analysis and Improvements for Incremental Nonlinear Dynamic Inversion Control". In: *2018 AIAA Guidance, Navigation, and Control Conference*. AIAA SciTech Forum. American Institute of Aeronautics and Astronautics, Jan. 2018. DOI: doi:10.2514/6.2018-1127. URL: https://doi.org/10.2514/6.2018-1127.

[11] et al. Jean-Jacques E Slotine Weiping Li. *Applied nonlinear control*. Ed. by Prentice hall Englewood Cliffs. 1st ed. Vol. 199. 1991.

[12] Daewon Lee, H Jin Kim, and Shankar Sastry. "Feedback linearization vs. adaptive sliding mode control for a quadrotor helicopter". In: *International Journal of Control, Automation and Systems* 7.3 (2009), pp. 419–428. ISSN: 1598-6446. DOI: 10.1007/s12555-009-0311-8. URL: https://doi.org/10.1007/s12555-009-0311-8.

[13] S Sieberling, Q P Chu, and J A Mulder. "Robust Flight Control Using Incremental Nonlinear Dynamic Inversion and Angular Acceleration Prediction". In: *Journal of Guidance, Control, and Dynamics* 33.6 (Nov. 2010), pp. 1732–1742. ISSN: 0731-5090. DOI: 10.2514/1.49978. URL: https://doi.org/10.2514/1.49978.

[14] Ewoud Smeur, Guido Croon, and Q Chu. "Cascaded Incremental Nonlinear Dynamic Inversion Control for MAV Disturbance Rejection". In: *Control Engineering Practice* 73C (Apr. 2018), pp. 79–90. DOI: 10.1016/j.conengprac.2018.01.003.

[15] Ewoud J J Smeur, Qiping Chu, and Guido C H E de Croon. "Adaptive Incremental Nonlinear Dynamic Inversion for Attitude Control of Micro Air Vehicles". In: *Journal of Guidance Control and Dynamics* 39 (2016), pp. 450–461.

[16] Ezra Tal and Sertac Karaman. "Accurate Tracking of Aggressive Quadrotor Trajectories Using Incremental Nonlinear Dynamic Inversion and Differential Flatness". In: *IEEE Transactions on Control Systems Technology* 29.3 (2021), pp. 1203–1218. DOI: 10.1109/TCST.2020.3001117.

[17] Ezra A Tal and Sertac Karaman. "Global Trajectory-tracking Control for a Tailsitter Flying Wing in Agile Uncoordinated Flight". In: *AIAA AVIATION 2021 FORUM*. AIAA AVIATION Forum. American Institute of Aeronautics and Astronautics, July 2021. DOI: doi:10.2514/6.2021-3214. URL: https://doi.org/10.2514/6.2021-3214.

[18] Ewoud Smeur, Murat Bronz, and Guido Croon. "Incremental Control and Guidance of Hybrid Aircraft Applied to a Tailsitter Unmanned Air Vehicle". In: *Journal of Guidance, Control, and Dynamics* (Feb. 2018). DOI: 10.2514/1.G004520.

[19] Stefan A Raab et al. "Consideration of Control Effector Dynamics and Saturations in an Extended INDI Approach". In: *AIAA Aviation 2019 Forum*. AIAA AVIATION Forum. American Institute of Aeronautics and Astronautics, June 2019. DOI: doi:10.2514/6.2019-3267. URL: https://doi.org/10.2514/6.2019-3267.

[20] Xiang Li et al. "A Method to Compensate Interaction between Actuator Dynamics and Control Allocator under Incremental Nonlinear Dynamic Inversion Controller". In: *IOP Conference Series: Materials Science and Engineering* 428 (Oct. 2018), p. 012048. ISSN:

1757-899X. DOI: 10.1088/1757-899X/428/1/012048. URL: https://iopscience.iop.org/article/10.1088/1757-899X/428/1/012048.

[21] Rasmus Steffensen, Agnes Steinert, and Ewoud Jan Jacob Smeur. "Non-Linear Dynamic Inversion with Actuator Dynamics: an Incremental Control Perspective". In: (Jan. 2022). DOI: 10.48550/arxiv.2201.09805. URL: http://arxiv.org/abs/2201.09805.

[22] Pranav Bhardwaj, Stefan A Raab, and Florian Holzapfel. "Higher Order Reference Model for Continuous Dynamic Inversion Control". In: *AIAA Scitech 2021 Forum*. AIAA SciTech Forum. American Institute of Aeronautics and Astronautics, Jan. 2021. DOI: doi:10.2514/6.2021-1130. URL: https://doi.org/10.2514/6.2021-1130.

[23] Pranav Bhardwaj et al. "Integrated Reference Model for a Tilt-rotor Vertical Take-off and Landing Transition UAV". In: *2018 Applied Aerodynamics Conference* (2018).

[24] Stefan A Raab et al. "Proposal of a Unified Control Strategy for Vertical Take-off and Landing Transition Aircraft Configurations". In: *2018 Applied Aerodynamics Conference*. AIAA AVIATION Forum. American Institute of Aeronautics and Astronautics, June 2018. DOI: doi:10.2514/6.2018-3478. URL: https://doi.org/10.2514/6.2018-3478.

[25] Florian Peter, Miguel Leitao, and Florian Holzapfel. *Adaptive Augmentation of a New Baseline Control Architecture for Tail-Controlled Missiles Using a Nonlinear Reference Model*. Aug. 2012. ISBN: 978-1-60086-938-9. DOI: 10.2514/6.2012-5037.

[26] Mehrdad Shademan and Arash Naghib-Lahouti. "Effects of aspect ratio and inclination angle on aerodynamic loads of a flat plate". In: *Advances in Aerodynamics* 2.1 (2020), p. 14. ISSN: 2524-6992. DOI: 10.1186/s42774-020-00038-7. URL: https://doi.org/10.1186/s42774-020-00038-7.

[27] P Simplício et al. "An acceleration measurements-based approach for helicopter nonlinear flight control using Incremental Nonlinear Dynamic Inversion". In: *Control Engineering Practice* 21.8 (2013), pp. 1065–1077. ISSN: 0967-0661. DOI: https://doi.org/10.1016/j.conengprac.2013.03.009. URL: https://www.sciencedirect.com/science/article/pii/S0967066113000634.

2

Literature Study

Contents

Nomenclature

Abbreviations

Abbreviation	Definition
PID	Proportional, Integral, Derivative
INDI	Incremental Nonlinear Dynamic Inversion
PCH	Pseudo Control Hedging
RM	Reference Model
EC	Error Controller

Symbols

Symbol	Definition	Unit
$\boldsymbol{x}(t)$	State Vector as Function of Time	-
$\boldsymbol{u}(t)$	Input Vector as Function of Time	-
$\boldsymbol{y}(t)$	Output Vector as Function of Time	-
$\boldsymbol{f}$	Nonlinear Plant Dynamics Vector	-
$\boldsymbol{h}$	Nonlinear Output Dynamics Vector	-
$\boldsymbol{\Delta u}$	Input Increment Vector	-
$\boldsymbol{G}(\boldsymbol{x}_0, \boldsymbol{u}_0)$	Control Effectiveness Matrix	-
$\boldsymbol{F}(\boldsymbol{x}_0, \boldsymbol{u}_0)$	State Effectiveness Matrix	-
$\boldsymbol{K}_R$	Reference Model Coefficients Vector	-
$\boldsymbol{K}_E$	Error Controller Coefficients Vector	-
$\boldsymbol{K}_{EI}$	Error Controller Integrator Coefficients Vector	-
$H^{\delta}_{u_{ideal}}(s)$	Transfer Function for Ideal Actuator	-
$\boldsymbol{n}_C$	Load Factor Vector in the Control Frame	-
$\boldsymbol{C}_v$	Selection Matrix for Virtual Control Inputs	-
$\boldsymbol{\nu}$	Pseudo Control Input Vector	-
$\boldsymbol{\xi}$	External Reference State Trajectory Vector	-
$\boldsymbol{\chi}$	Deviation in Reference State Trajectory	-
Δ_x	State Dependent Increment Term	-
Δ_u	Control Dependent Increment Term	-
$\dot{\boldsymbol{\omega}}$	Body Angular Accelerations Vector	-

List of Figures

1 Introduction

In the past two decades, unmanned air vehicles (UAVs) became increasingly relevant for humanity. As of today, drones are being employed for a wide spectrum of operations and purposes, from inspection to delivery, to even entertainment. The investments and global interest in the field is in constant growth [8], and with it the demand of more challenging operations. The scientific advancements however seems not able to perfectly keep up with the demanding industry, which asks for performances that are not yet achievable by the present day technology, for example landing on a moving ship [9]. This is caused by several factors, such as hardware, aerodynamics and control. This project's area of interest is the latter, which represents a field in constant evolution and expansion thanks to the existence of UAVs. More in detail, it focuses on a particular control strategy referred as Incremental Nonlinear Dynamic Inversion (INDI) [26], which in the past decade caused a great interest in the scientific community due to its simplicity and robustness to disturbances respect to conventional PID solutions [29]. In the years, several limitations in this strategy have been found, which degrade the overall performance of the commanded vehicle, especially in certain scenarios, mainly two: when the vehicle presents non-ideal or uncoupled actuators and when the trajectory to be tracked demands aggressive accelerations. Together with the discovery of such, the scientific community worked towards expansions of the conventional INDI strategy to solve these issues.

The main advancements in the mitigation of these limitations mainly focused on keeping the simplicity of INDI intact. [21] proposed a new method to include actuator dynamics in the loop, improving the performance for cases where actuators are slow. [4] developed a scheme to improve the trajectory tracking while high accelerations are demanded. With the use of differential flatness [11], [32] managed to develop an INDI controller that fully exploited the capabilities of the considered tailsitter drone. Many unsolved issue however still remains, as the current solutions do not take into account external disturbances, a major threat in outdoor operations, and have not been tested or validated in outdoor environments.

This project then wants to expand INDI by using model information to tackle the issues originated from the uncertainties of the outdoor environment. Based on the current advancements, the goal is therefore to look at how these can contribute to the disturbance rejection of the vehicle as well. In addition to that, since many methods mentioned did not provide validation outdoor, this work aims to provide more clarity on what are the real capabilities of these and how can be made more robust. The final outcome is therefore to obtain a global INDI controller that presents clear performance improvements both in tracking and disturbance rejection in outdoor environments.

The search for a uniform model based INDI control strategy will therefore be structured as follows. The work starts in Chapter 2 with the formulation of the research plan for this literature study. In Chapter 3 an introduction to INDI control is provided. Chapter 4 further expands the knowledge available about INDI by focusing on the limitations that this strategy presents in determinate conditions. In Chapter 5, a detailed overview on how the scientific field developed solutions to compensate with the mentioned limitations is provided. For a better assessment on the validity and the potential of such solutions,

Chapter 6 examines their effect in a simulated environment and draws preliminary conclusions on which direction should be taken to further improve the current methods. Chapter 7 then further expands the research plan formulated in Chapter 2 based on the findings of the literature study, and builds a more complete and accurate research plan for the upcoming thesis work. The report finally ends with Chapter 8, where conclusive remarks are provided with an overview of the work conducted.

2

Research Plan Literature Study

As already mentioned in the introduction, this thesis focuses on the realization of a model-based extension of the conventional INDI control strategy. This is the most promising way to develop INDI towards a more global control strategy. The research objective that can be formulated upon such notion is then the following:

To achieve an INDI-based control strategy that takes into account conventional INDI limitations by including model terms and actuator dynamics into the controller design.

The objective posed here touches a various and quickly evolving body of knowledge, which must be fully understood and assessed to understand what to target and how.

The literature study therefore starts by explaining INDI, including its core structure, its predecessors and its advantages from other controller solutions. A complete overview of this control strategy is required to then assess the nature of the limitations mentioned. A limitation in a controller means that for a realistic and specific scenario, it will fail in operating as desired. The questions to answer in this regards therefore ask when INDI fails, and why. The work exposed here provides a full overview of the scenarios where INDI controllers do not perform as they should, where a scenario includes the type of platform used and the type of flight path encountered. Particular focus is also dedicated towards the reasons of such drawbacks. Efforts are made in providing a mathematical as well as practical overview of the flaws that characterize this controller in the scenarios mentioned.

Once a body containing the advantages and limitations or INDI controllers is concluded, the focus can be directed towards the efforts made by scientists in order to compensate for these. It has already been mentioned that the solution proposed in this thesis is model-based, but no information is available so far regarding the nature of such compensation. The reason for this is that a wide span of techniques have been used, but these target a limited number of limitations on few scenarios. The objective here is then to understand which recent breakthrough has more potential to be expanded to a more global application. A detailed assessment is therefore made around this.

To fully understand the entity of the different drawbacks that revolve around INDI controllers, but also the validity of some solutions, the assessment conducted around this work is supported by simulation results obtained from an existing model of the F-16 fighter aircraft, provided by [25].

The knowledge provided in this body of work is expected therefore to answer the research question, put as:

To what extent can the deviation error in trajectory tracking using INDI be compensated for by means of model-based solutions and actuator dynamics considerations, and how?

3

Incremental Nonlinear Dynamic Inversion

Since the introduction of the first aircraft, efforts have been made in the design of robust and cost effective control strategies. So far, many certified and operating passenger aircraft operate by means of conventional proportional, integral, derivative (PID) control. Due to the high number of flight phases contained in the flight envelope of an aircraft, and therefore the consequent introduction of nonlinearities required for the description of the full system, PID control is often extended by means of gain scheduling. Such practice requires substantial work of tuning which remains applicable only to the aircraft considered in the design of the controller. In the field of scaled UAVs, such practice is not applicable, as airframe configurations differ vastly compared to passenger aircrafts, and low costs and faster implementation are a strict requirement.

In the light of this, model based control techniques were developed. It was found that the partial knowledge of the aerodynamics of a specific vehicle can tackle the adaptation to nonlinearities with a much smaller effort compared to PID gain scheduling [28]. This concept is best expressed with the nonlinear dynamic inversion (NDI) control strategy, which relies on the linearization of the aircraft aerodynamics to derive the most optimal control input. Such technique proves to be effective, except in situations where the model does not match reality. This turns out to be a relevant issue, as UAVs usually present configurations that are hard to model accurately, making NDI not robust in too many scenarios. The logical step forward is to therefore reduce model dependency.

3.1. Reduction of Model Dependency Through Incremental Control

A first attempt in reducing dependency on the aerodynamic model is made by [3], where the control objective consists in obtaining the required input for trajectory tracking given limited model information. This work laid the base for the first design of incremental nonlinear dynamic inversion control [26], which is summarized in the following pages.

For this overview, a nonlinear system as in Equation 3.1 below is considered.

$$\begin{aligned} \dot{\boldsymbol{x}}(t) &= \boldsymbol{f}(\boldsymbol{x}(t), \boldsymbol{u}(t)) \\ \boldsymbol{y}(t) &= \boldsymbol{h}(\boldsymbol{x}(t)) \end{aligned} \tag{3.1}$$

With $\boldsymbol{x}(t) \in \mathbb{R}^{n_x}$ the state vector, $\boldsymbol{u}(t) \in \mathbb{R}^{n_u}$ the input vector and $\boldsymbol{y}(t) \in \mathbb{R}^{n_y}$ the output vector. For simplicity, the term (t), which indicates the dependency in time of the vectors mentioned, is omitted for the rest of this work. $\boldsymbol{f}_{n_x \times 1} : D_{x,\boldsymbol{u}} \rightarrow \mathbb{R}^{n_x}$ represents then the nonlinear plant dynamics and $\boldsymbol{h}_{n_y \times 1} : D_{\boldsymbol{x}} \rightarrow \mathbb{R}^{n_y}$ the output dynamics. The objective of NDI is to linearize the plant dynamics around the current state and input to then perform a linear inversion with the goal of obtaining an expression

for the input vector $\boldsymbol{u}$. Linearization is carried over by means of Taylor series expansion around the current state in Equation 3.2.

$$\begin{aligned}\dot{\boldsymbol{x}} &\simeq \boldsymbol{f}(\boldsymbol{x}_0, \boldsymbol{u}_0) + \left.\frac{\partial \boldsymbol{f}(\boldsymbol{x}, \boldsymbol{u})}{\partial \boldsymbol{x}}\right|_{\boldsymbol{x}=\boldsymbol{x}_0, \boldsymbol{u}=\boldsymbol{u}_0} (\boldsymbol{x} - \boldsymbol{x}_0) + \left.\frac{\partial \boldsymbol{f}(\boldsymbol{x}, \boldsymbol{u})}{\partial \boldsymbol{u}}\right|_{\boldsymbol{x}=\boldsymbol{x}_0, \boldsymbol{u}=\boldsymbol{u}_0} (\boldsymbol{u} - \boldsymbol{u}_0) \\ \dot{\boldsymbol{x}} &\simeq \dot{\boldsymbol{x}}_0 + \underbrace{\boldsymbol{F}(\boldsymbol{x}_0, \boldsymbol{u}_0)(\boldsymbol{x} - \boldsymbol{x}_0)}_{\Delta_x} + \underbrace{\boldsymbol{G}(\boldsymbol{x}_0, \boldsymbol{u}_0)(\boldsymbol{u} - \boldsymbol{u}_0)}_{\Delta_u}\end{aligned} \tag{3.2}$$

Where the second term represents the state dependent increment Δ_x and the third term is the control dependent increment Δ_u, which together fully describe the vehicle dynamics. To reach the conventional INDI controller expression, its however required to neglect the second term, which is representative of the vehicle dynamics. The neglection of the state dependent increment Δ_x is based on the principle of time scale separation [27]; as visible from Equation 3.2, the control input $\boldsymbol{u}$ has an instantaneous effect on the state change vector $\dot{\boldsymbol{x}}$. On the other hand, Δ_x is dependent on the state vector $\boldsymbol{x}$, which is obtained by an integration of $\dot{\boldsymbol{x}}$, which results in a slower change. Assuming that the commanded value achieves the desired state change instantaneously (in other words, the system is equipped with infinitely fast actuators) and that the state is fed back to the controller with zero time delay, in a small time interval the "slow" state dynamics can be assumed as constant, leading to a negligible Δ_x. Based on the aforementioned, the plant dynamics can be simplified to

$$\dot{\boldsymbol{x}} \simeq \dot{\boldsymbol{x}}_0 + \boldsymbol{G}(\boldsymbol{x}_0, \boldsymbol{u}_0)(\boldsymbol{u} - \boldsymbol{u}_0) = \dot{\boldsymbol{x}}_0 + \boldsymbol{G}(\boldsymbol{x}_0, \boldsymbol{u}_0)\Delta\boldsymbol{u} \tag{3.3}$$

where $\Delta\boldsymbol{u}$ is the control input increment. Equation 3.3 can then be rearranged to express the control increment in terms of the state and the of the plant, as in Equation 3.4.

$$\Delta\boldsymbol{u} = \boldsymbol{G}(\boldsymbol{x}_0, \boldsymbol{u}_0)^{-1}(\dot{\boldsymbol{x}} - \dot{\boldsymbol{x}}_0) \tag{3.4}$$

Given that a direct expression of the output $\boldsymbol{y}$ in function of the input $\boldsymbol{u}$ can be found, the obtained equation can then be expressed in terms of the output vector, which represents the trajectory to be tracked. The system considered here is assumed to have a relative degree r of 1. This means that only one derivation of the output is required to to obtain a direct relation between the desired control variable and the control input. Based on this assumption, the following is true

$$\begin{aligned}\boldsymbol{y} &= \boldsymbol{h}(\boldsymbol{x}) = \boldsymbol{x} \\ \dot{\boldsymbol{x}} &= \dot{\boldsymbol{y}} \\ \boldsymbol{\nu} &= \dot{\boldsymbol{y}} = \dot{\boldsymbol{x}}\end{aligned} \tag{3.5}$$

Where $\boldsymbol{\nu}$ represents the pseudo control input of the controller. Equation 3.4 can then be reformulated as follows

$$\Delta\boldsymbol{u} = \boldsymbol{G}(\boldsymbol{x}_0, \boldsymbol{u}_0)^{-1}(\boldsymbol{\nu} - \dot{\boldsymbol{x}}_0) \tag{3.6}$$

which represents the conventional INDI control law. This includes the effectiveness matrix $\boldsymbol{G}(\boldsymbol{x}_0, \boldsymbol{u}_0)^{-1}$, the pseudo control input $\boldsymbol{\nu}$, extracted from the desired trajectory, and the current state $\dot{\boldsymbol{x}}_0$, estimated by on board sensors. A visual representation of the described control law can be found in Figure 3.1.

3.2. Reference Model for Smooth Trajectory Generation

It is not always the case, however, that the system to be controlled has a relative degree r of 1. For scenarios where the relative degree is higher, the pseudo control input becomes the r^{th} derivative of the desired control output. In the case where a specific trajectory has to be tracked, this requirement introduces the need to generate smooth and feasible trajectories that can be differentiated r times from the desired control trajectory. In INDI control design, this conversion can be computed by reference

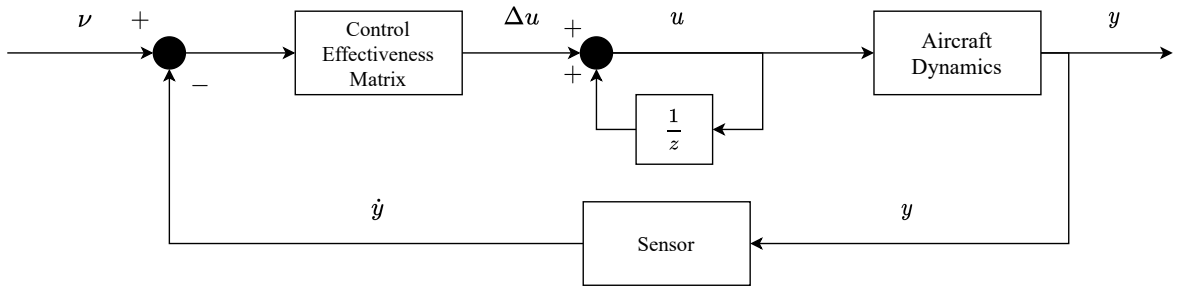

Figure 3.1: Conventional INDI control scheme

models [20]. Despite the wide range of reference models available for trajectory generation [5, 4, 23], the general structure for an arbitrary relative degree r can be summarized in Figure 3.2.

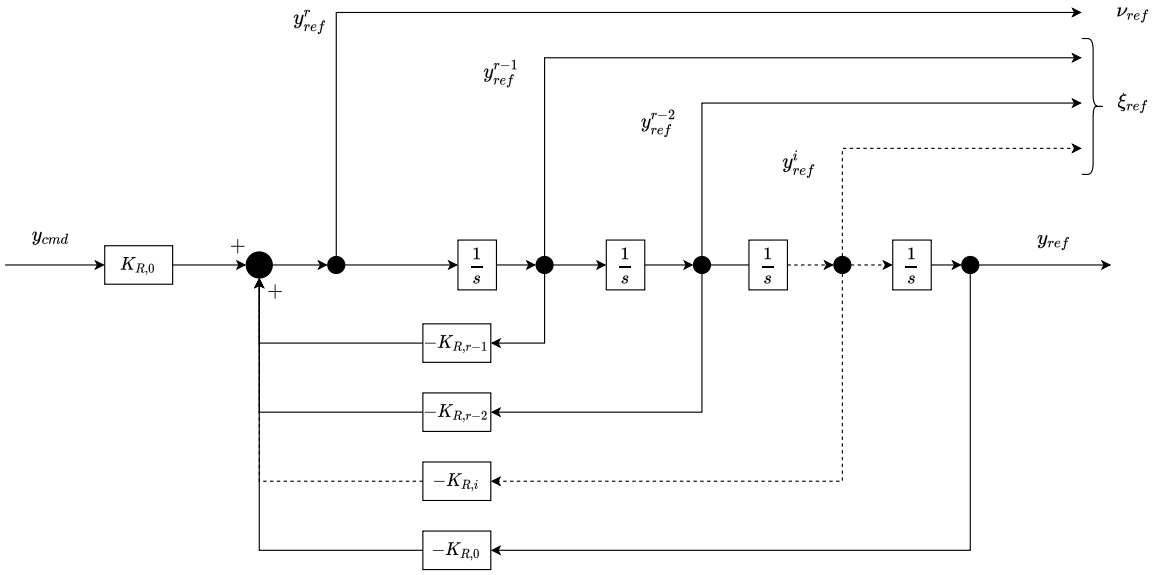

Figure 3.2: Linear reference model for an arbitrary relative degree r (from [4])

The coefficients vector $\boldsymbol{K}_R \in \mathbb{R}^r$ is selected such that the higher order derivatives of the desired output generate physically feasible trajectories [4].

The importance of the reference model in INDI control is also due to the fact that it does not only provide the pseudo control input $\boldsymbol{\nu_{ref}}$, but also information related to the reference trajectories of the states not directly tracked by the INDI loop (i.e. the lower order derivatives of $\boldsymbol{\nu_{ref}}$). This vector is commonly referred as $\boldsymbol{\xi_{ref}}$, or external reference state trajectory. The availability of such information is fundamental for INDI tracking augmentation, as discussed in the following section.

3.3. Error Controller for Disturbance Rejection

The INDI loop, as shown in Figure 3.1, is responsible for tracking the pseudo control input $\boldsymbol{\nu_{ref}}$ only, without knowing whether or not the tracking is causing a deviation in the lower level derivatives of $\boldsymbol{\nu_{ref}}$, and eventually the control command. Knowledge of the external reference state trajectory $\boldsymbol{\xi_{ref}}$ is therefore required to compensate for deviations. This compensation usually performed through the introduction of an error controller (EC) [22]. The controller looks at the deviation of the current external reference state $\hat{\boldsymbol{\xi}}$ (which contains the lower order derivatives of the pseudo control input vector) from the reference trajectory $\boldsymbol{\xi_{ref}}$, defined as

$$\boldsymbol{\chi} = \boldsymbol{\xi_{ref}} - \hat{\boldsymbol{\xi}} \tag{3.7}$$

where χ represents the deviation of all n_y output channels. For an easier understanding, only the first channel is considered. The deviation χ^1 of the first output channel is multiplied by a row of coefficients $(\boldsymbol{K}_E^T)_1$ which, like in the reference model, are selected to meet the physical limitations of the vehicle. In addition, an integral feedback of the output error can be added to compensate for steady state errors [22] (see Section 6.3.3). The obtained pseudo control compensation $\boldsymbol{\nu_{1,ec}}$ is then added to the pseudo control input $\boldsymbol{\nu_{1,ref}}$ generated by the reference model and fed to the INDI closed loop. Figure 3.3 shows schematically the process for the first output channel.

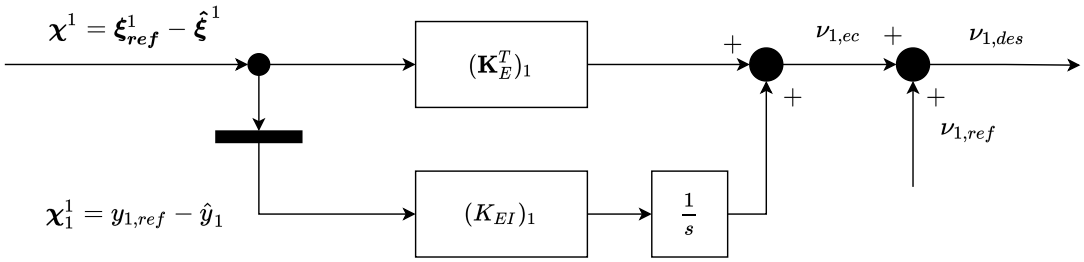

Figure 3.3: Error controller used in INDI applications for deviation compensation [21]

3.4. Conventional INDI Controller Structure

With the addition of the error controller and the reference model, an INDI based controller, in ideal conditions, is able to track the predefined trajectory without the need of model knowledge. Given a desired output, the reference model is responsible to provide a smooth trajectory for higher order derivatives of that output up to the pseudo control input order. It also provides, if any, the intermediate derivatives. The error controller is responsible to compensate for the neglection of the state dependent increment term and to cope with external disturbances by comparing the external reference states with the real plant states and add such information to the pseudo control input. Based on the above, it is now possible to understand the conventional structure of an INDI controller, shown as block diagram in

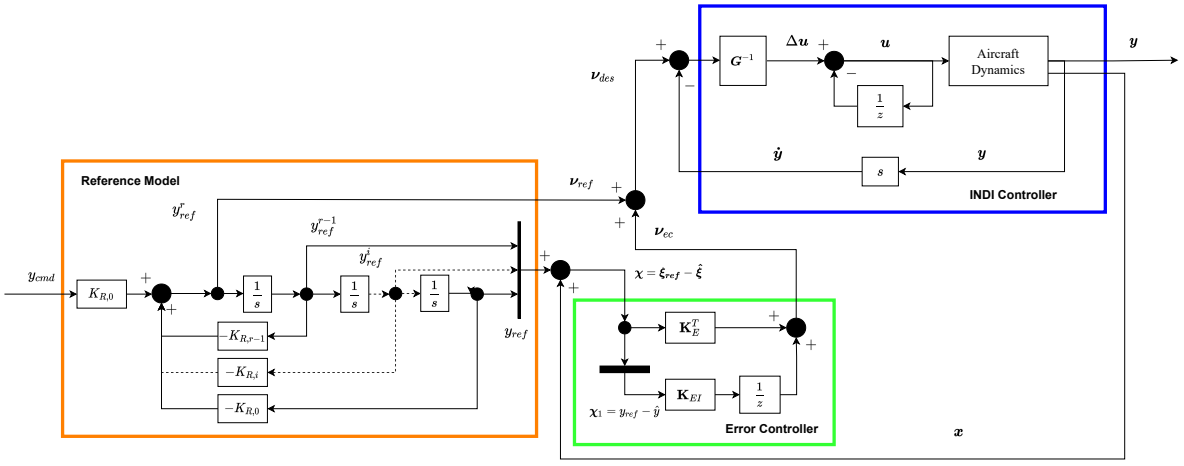

Figure 3.4: INDI controller with conventional reference model and error controller

As already mentioned in Section 3.1, the robustness of such strategy fails in certain limit conditions. The next section identifies the conditions and explains the types of failure.

4

Limitations in INDI Control

In Chapter 3 the neglection of the state dependent increment term Δ_x is a key factor for the simplicity and robustness of INDI controllers. However, this is based on some assumptions mentioned already. What happens when such assumptions do not hold? In what conditions do these assumptions fail? Researchers have, since the introduction of INDI, focused on the identification and understanding of such flaws, and placed them in an operational context, which is what this chapter is aiming to do.

4.1. Time Delay

In the real world, controllers achieve state estimation by means of sensors mounted on the vehicle. A sensor can be generalized as a device that observes the surrounding operating environment, measures one or more state variables (e.g. a gyro estimates rotational velocities around 3-axis) and communicates the magnitude of the measured state to the autopilot. Such operation is not instant: each sensor is characterized by a certain time delay. In addition, every sensor, even the most accurate ones, provides a measurement signal characterized by the presence of certain amount of noise. Since the feedback requires differentiation, such noise is amplified [30]. The use of a second order filter is usually employed for noise reduction [2]. Filtering induces lag, and therefore additional delay.

Delay in sensor measurement becomes and issue when it is not equally delayed with the actuator measurements, leading to more instability [1]. Mathematically, a delay would mean that the control law in Equation 3.6 is now affected by a delayed measurement $\dot{\boldsymbol{x}}_\tau$, leading to

$$\Delta \boldsymbol{u} = \boldsymbol{G}(\boldsymbol{x}_0, \boldsymbol{u}_0)^{-1}(\boldsymbol{\nu} - \dot{\boldsymbol{x}}_\tau) \tag{4.1}$$

If Equation 4.1 is used in for the expression of the simplified system in Equation 3.3, the cancellation is not perfect

$$\begin{aligned} \dot{\boldsymbol{x}} &\simeq \dot{\boldsymbol{x}}_0 + \boldsymbol{G}(\boldsymbol{x}_0, \boldsymbol{u}_0)\boldsymbol{G}(\boldsymbol{x}_0, \boldsymbol{u}_0)^{-1}(\boldsymbol{\nu} - \dot{\boldsymbol{x}}_\tau) \\ \dot{\boldsymbol{x}} &\simeq \boldsymbol{\nu} + \dot{\boldsymbol{x}}_0 - \dot{\boldsymbol{x}}_\tau \\ \dot{\boldsymbol{x}} &\simeq \boldsymbol{\nu} + \dot{\boldsymbol{x}}_{\Delta\tau} \end{aligned} \tag{4.2}$$

The term $\dot{\boldsymbol{x}} \simeq \boldsymbol{\nu} + \dot{\boldsymbol{x}}_{\Delta\tau}$, the difference in state derivative in within the delay, is now affecting the tracking accuracy of the controller, which may lead to instability for certain time spans.

4.2. Actuator Dynamics

As already mentioned, an assumption on which INDI bases its simplicity is the neglection of actuator dynamics [26]. Actuators considered in INDI applications are therefore considered as instantaneous, with no limitations in position and rate. This means that the transfer function between the commanded input and the actual input sent to the aircraft dynamics is 1

$$\begin{aligned} u &= H^{\delta}_{u_{ideal}}(s) \cdot u_{cmd} = u_{cmd} \\ H^{\delta}_{u_{ideal}}(s) &= 1 \end{aligned} \tag{4.3}$$

Which means that the actuator can perfectly track the control command obtained from the inversion. In reality however, actuators present non-linear dynamics of first or second order, together with position and rate limits. In a number of scenarios, such omission can lead to bad tracking, or even instability [15, 19].

One example is the scenario where actuators are slow and cannot track a trajectory in time. The settling time for the actuator is too large and a change in trajectory cannot be followed with the optimal control commands. In addition, neglection of rate and position limits can lead to saturation [1].

In most cases, for example while operating a quadrotor [10], this deficit does not constitute an issue, and the vehicle can still perform well. This is because the dynamics of the actuators used on such UAVs are much faster than their rotational dynamics. The same cannot be asserted for drones such as transition or fixed wing vehicles. Given the increasing relevance of such configurations in the past years, the issue cannot be ignored.

4.3. Agile Maneuvering

INDI takes its simplicity and ease of implementation from the neglection of the state dependent increment Δ_x. This is justified by the fact that the sample rate is high and the acceleration dynamics being controlled directly by the control command are faster than the velocities, which are described by

$$\begin{aligned} \boldsymbol{x}_{cmd} &= \dot{\boldsymbol{x}}_0 + \boldsymbol{G}(\boldsymbol{x}_0, \boldsymbol{u}_0)\Delta \boldsymbol{u}_{cmd} \\ \boldsymbol{x}_e &= \boldsymbol{x}_{des} - \boldsymbol{x}_{cmd} = \boldsymbol{F}(\boldsymbol{x}_0, \boldsymbol{u}_0)\Delta \boldsymbol{x} = \Delta_x \end{aligned} \tag{4.4}$$

Where $\boldsymbol{x}_{des}$ represents the ideal pseudo control input (therefore the pseudo control input obtained by a perfect NDI controller) and $\boldsymbol{x}_{cmd}$ is the pseudo control input that does not include the state dependent term. $\boldsymbol{x}_e$ propagates then through the chain of integrators of the reference model, causing an error. In some scenarios such error does not badly deteriorate the trajectory tracking, and the error controller can compensate well for it. On the other hand, if scenarios such as the one mentioned in Chapter 1 are considered, $\boldsymbol{x}_e$ must be compensated based on the real capabilities of the vehicle. The task of following a moving ship and autonomously land on a narrow, moving space [9] requires an accurate tracking of a continuously morphing trajectory. Quick changes in position setpoints bring to high acceleration, and therefore a quick change in $\Delta \boldsymbol{x}$. The increasing complexity in drone operations makes this an important issue to be considered in extended INDI controller designs.

4.4. Flight Phase Transition

Dynamic inversion based controllers require a usable trajectory that can be followed to perform the inversion. For example, in an INDI based tracking of angular acceleration, a feasible acceleration path must be provided to obtain the required controls. This is usually done via a reference model, as mentioned in Section 3.2, which linearly derives the pseudo control input value required for the inversion.

A linear, conventional reference model therefore does not generate a trajectory that takes into account the strong change in vehicle dynamics that occurs when a flying vehicle undergoes a change in flight phase, such as a switch from vertical hovering to horizontal flight [6]. This can cause the generation of a practically infeasible trajectory and a degradation of performance [5]. Transition UAVs are increasing in use because of their excellent performance both in hover and forward flight, which makes the consideration of flight phase another issue to be considered.

4.5. Disturbance Load Alleviation

The reference model, linear or nonlinear, provides a trajectory to be followed to reach the control objective. The controller is then responsible for providing the right control inputs to remain on track. In

reality, model mismatch or external disturbances (such a collision or a gust of wind), temporarily introduce a large deviation of the drone states from the reference trajectory. In a default scenario, the error controller mentioned in Section 3.3 adds a correction signal to the ideal pseudo control input based on the magnitude of the deviation encountered.

Despite the good response of the conventional controller, it is clear however how the compensation is carried over by a simple linear error controller that does not provide a new optimal rerouting of the trajectory to get back on track, but simply indicates the error. In other words, the reference model is not able to provide a suitable solution to reestablish perfect tracking, because it does not know what the current state is. If such knowledge would be made available to a RM that generates trajectories that exploit the full capabilities of the vehicle, more efficient commands can be generated and best performance can be achieved.

5

Model Based Compensation of INDI Limitations

As discussed previously in Chapter 4, it is clear that the INDI controller as proposed in [26] cannot be used for a wide span of scenarios. In addition, given the increasing complexity in drone operations and mission in the last years, many issues must be fixed to make such control strategy competitive and benefit from its main advantages.

In the past years, scientists identified the mentioned issues and developed a various number of solutions which targeted one or more of these with different methods, applied on different locations of the INDI structure of Chapter 3. The role of this section is to gather the most relevant and promising advancements in INDI and understand their potential, to then build a global compensation strategy.

5.1. Differential Flatness Transform

Differential flatness is a property of a certain subgroup of systems (flat systems) which has shown great potential in nonlinear control application in the past decades [13]. The first cases of differential flatness on UAVs can be found on quadrotors [7, 17], while only recently has been applied on different, more complex configurations [31].

Such technique is particularly attractive for nonlinear control application for one major property. Given a flat system, it is always possible to express the input and state of the system in terms of the output and a finite number of its derivatives [12]. Mathematically, given a system

$$\dot{\boldsymbol{x}} = \boldsymbol{f}(\boldsymbol{x}, \boldsymbol{u}) \tag{5.1}$$

where $\boldsymbol{x} \in \mathbb{R}^n$ is the state vector, $\boldsymbol{u} \in \mathbb{R}^m$ is the input vector and $\boldsymbol{y} \in \mathbb{R}^m$ the flat output vector, if the system is flat, then the following vectors of equations exist

$$\begin{aligned} \boldsymbol{y} &= \boldsymbol{h}(\boldsymbol{x}, \boldsymbol{u}, \dot{\boldsymbol{u}}, \dots, \boldsymbol{u}^{(r)}) \\ \boldsymbol{x} &= \boldsymbol{\theta}(\boldsymbol{y}, \dot{\boldsymbol{y}}, \dots, \boldsymbol{y}^{(q)}) \\ \boldsymbol{u} &= \boldsymbol{\gamma}(\boldsymbol{y}, \dot{\boldsymbol{y}}, \dots, \boldsymbol{y}^{(q)}) \end{aligned} \tag{5.2}$$

Where q represents the relative degree of the system, which is always smaller or equal than the order n of the system. More information on the identification of flat systems can be found in [24].

The property stated is excellent for trajectory tracking purposes, as it allows for direct derivation of of the input and state trajectories from the output trajectory. Differential flatness transform is therefore used for feed-forward control terms generation [10]. Its property allows to avoid linearization of the model dynamics, which is usually performed in INDI applications (see Equation 3.2), to perform the inversion.

No simplification, such as in Equation 3.3, is required and all the nonlinearities that characterize a complex system are maintained [32].

The advantages brought by differential flatness transform in INDI control are therefore mainly three, listed below:

- **Conservation of nonlinearities**: flight phases transitions and agile maneuvers are complicated to express in a linear fashion. By avoiding linearization, a better representation of these maneuvers is possible.
- **Reduction of hardware complexity**: since the dynamics of the system are expressed in term of less variables, it becomes easier to generate a trajectory, since the reference model incorporates less variables for the generation of the pseudo control input, and the actual plant needs to feed back measurements of fewer states. This means that the vehicle would require less sensors.
- **Tracking of high level derivatives**: given the composition of the inverted equations, it becomes possible to track derivatives of the position or orientations of a selected UAV higher than the acceleration. This provides more information on the trajectory and allows for a better response to rapid changes. Trajectory tracking of such derivatives has proven its relevance in practice through the employment of jerk tracking [32] or even snap [17].

Differential flatness transform has been therefore proven to be highly efficient in the context of agile trajectory tracking. With the preservation of the model dynamics, the state dependent error mentioned in Section 4.3 is compensated.

However, no research has been conducted on differential flatness based vehicle control with actuator consideration. [24] researched flatness based actuator control by proposing a method to control an actuator of unknown model or characterized by non measurable variables, but this investigation is limited to the actuator itself, and not incorporated in the control of the vehicle. As already discussed in Section 4.2, actuator consideration is an obligatory step to achieve a complete extension of the INDI controller. In addition, control of flat systems is usually tackled by maintaining an equal number of flat outputs and control input commands, as only one control solution can be obtained instead or running an optimisation process that would slow down the control loop. This might pose a problem in the context of over-actuated flying vehicles, which is a scenario so far not considered in literature.

5.2. Virtual Control Inputs

The greatest issue related to the control of transitioning vehicles is that they have different flight phases in their operational envelope: this entails a profound change in vehicle dynamics between flight phases (for example between vertical landing and forward flight). If the intention is to design a global controller for the whole operational flight envelope of a vehicle, this can lead to complications.

The selection of pseudo control inputs in INDI controllers is usually carried over such that the control actuators are directly related to the degree of the state considered by the pseudo control input. In a conventional aircraft, for example, elevator deflections directly affect the angular acceleration, which is the reason why it is often used as a pseudo control input. This arrangement allows the actuators to be considered as ”fast”, enabling the neglection of the slower state increment term, as shown in Section 3.1.

Between flight phases, the same pseudo control input might become indirectly related to the control actuators, making them ”slow” and cause of transient errors. A good example can be found in [22]. There, the following pseudo control input is selected for the global INDI controller of a VTOL transition UAV with tilting rotors that allow vertical take-off and landing and forward flight

$$\boldsymbol{\nu}_{ref} = \begin{bmatrix} \boldsymbol{n}_C \\ \dot{\boldsymbol{\omega}} \end{bmatrix}_{ref} \tag{5.3}$$

where $\boldsymbol{n}_C \in \mathbb{R}^3$ is the load factor along all three axis of the control frame and $\dot{\boldsymbol{\omega}} \in \mathbb{R}^3$ are the body angular accelerations. In hover condition, the rotors directly affect $\boldsymbol{n}_C$, and considered as ”fast”. However, in forward flight, the major contributor to the vertical load factor is aerodynamic lift, which is directly

related to the angle of attack. Now the rotors can affect lift by directly changing the pitch rate, which builds up the angle of attack via two integrations. This increases the relative degree of the system by two. The assumption of the actuators to be ”fast” becomes then invalid.

A solution to such increase in relative degree would be to track the second derivative of the load factor $\ddot{n}_C$ trough dynamic extension [14]. In reality, feeding back estimations of the second derivative of the load factor is almost impossible, due to the high quantity of noise that characterizes this quantity.

As an alternative, [22] introduces the concept of virtual control input (VCI) $\boldsymbol{y}_v$, which is simply the selection of certain states from the state vector $\boldsymbol{x}$, through the selection matrix $\boldsymbol{C}_v$

$$\boldsymbol{y}_v = \boldsymbol{C}_v \cdot \boldsymbol{x} \tag{5.4}$$

It can be proven (see [22]) that the Jacobian $\boldsymbol{A}_{y_v}$ of $\dot{\boldsymbol{y}}$ (the pseudo control input vector) with respect to $\boldsymbol{y}_v$

$$\boldsymbol{A}_{y_v} = \left.\frac{\partial \boldsymbol{f}(\boldsymbol{x},\boldsymbol{u})}{\partial \boldsymbol{y}_v}\right|_{\boldsymbol{x}=\boldsymbol{x}_0,\boldsymbol{u}=\boldsymbol{u}_0} \tag{5.5}$$

can be used to obtain the vector

$$\begin{bmatrix}\Delta \boldsymbol{y}_v \\ \Delta \boldsymbol{u}\end{bmatrix} = \left(\begin{bmatrix}\boldsymbol{A}_{y_v} & \boldsymbol{G}_0\end{bmatrix}\right)^{-1} \cdot \Delta \dot{\boldsymbol{y}} = \left(\begin{bmatrix}\boldsymbol{A}_{y_v} & \boldsymbol{G}_0\end{bmatrix}\right)^{-1} \cdot \Delta \boldsymbol{\nu} \tag{5.6}$$

where $\boldsymbol{G}_0$ is the effectiveness matrix and $\boldsymbol{\nu}$ is the general notation used to express the pseudo control input. Equation 5.6 now presents the control input increment together with the virtual control input increment. $\boldsymbol{y}_v$ can be selected to be the direct actuator of the pseudo control input at a certain flight phase (e.g. the pitch angle, referring to the VTOL example) and used to compensate for the transient.

The virtual control input increment can then be fed to the reference model of the controller [5] for a trajectory generation that compensates for the induced transient errors (see Figure 5.1). Referring to the previous example with the VTOL, the pitch angle θ can be selected from the state vector to be a virtual control input. The pitch control increment is then expected to be non-zero during forward flight operation, therefore having a compensating effect when fed to the reference model for trajectory generation.

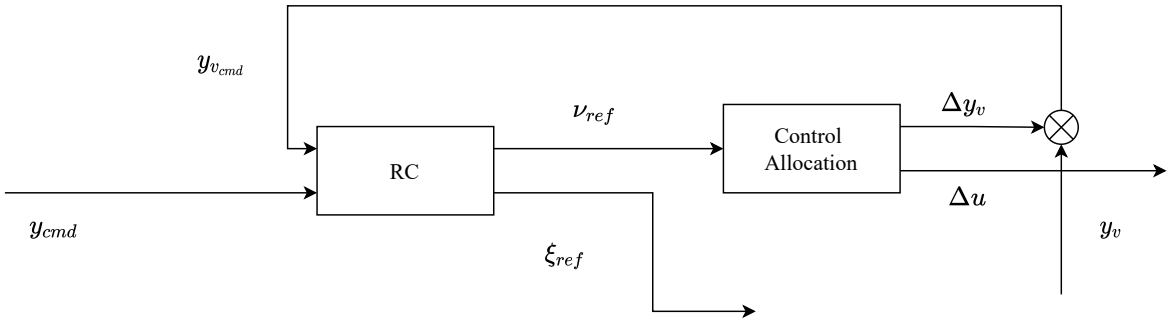

Figure 5.1: Virtual control input compensation [22]

The introduction of VCI in an INDI controller can therefore be beneficial for transitioning vehicles. It should be noted however, as clear from Figure 5.1, that the control allocation block now depends on its own output directly. Such recursion might eventually lead to instability, and should be therefore analysed further.

5.3. Actuator Compensation

As previously stated, both NDI and INDI were designed without taking into considerations the dynamics of actuators. If these are not taken into account, especially when actuators are slow, the tracking performance degrades and can even lead to instability [27].

5.3.1. Pseudo Control Hedging

A common compensation developed to alleviate the degrading effect is referred to as Pseudo Control Hedging (PCH) [1, 16]. PCH is meant to modify the pseudo control input generated by the reference model in case of actuator saturation in the plant. In a scenario where the actuator used for vehicle control saturates, the commanded control input $\boldsymbol{u}_{cmd}$ and the actual control input delivered to the plant dynamics $\boldsymbol{u}$ are different. This means that there is a deviation from the pseudo control input $\boldsymbol{\nu}$. However, if the model for the estimation of the pseudo control input is known, an estimate $\hat{\boldsymbol{\nu}}$ of the actual pseudo control input can be obtained. For the case of INDI control

$$\begin{aligned} \hat{\boldsymbol{\nu}} &= \dot{\boldsymbol{x}}_0 + \boldsymbol{G}(\boldsymbol{x}_0, \boldsymbol{u}_0)\Delta\boldsymbol{u} \\ \boldsymbol{\nu} &= \dot{\boldsymbol{x}}_0 + \boldsymbol{G}(\boldsymbol{x}_0, \boldsymbol{u}_0)\Delta\boldsymbol{u}_{cmd} \\ \Delta\boldsymbol{u} &= \boldsymbol{A}(s)\Delta\boldsymbol{u}_{cmd} \\ \hat{\boldsymbol{\nu}} &\neq \boldsymbol{\nu} \end{aligned} \tag{5.7}$$

Where the difference between the estimate and the ideal signal is referred to as hedging signal

$$\boldsymbol{\nu}_h = \hat{\boldsymbol{\nu}} - \boldsymbol{\nu} \tag{5.8}$$

The hedging signal increases as the actuators saturate and are not able to follow the trajectory anymore. For this reason, $\boldsymbol{\nu}_h$ is fed into the reference model for compensation of the following pseudo control input, as shown in Figure 5.2. Usually, given inversion uncertainties, the hedging signal is sent for compensation only when the commanded and actual control inputs differ [16]. This requires the addition of a logic controller in the loop.

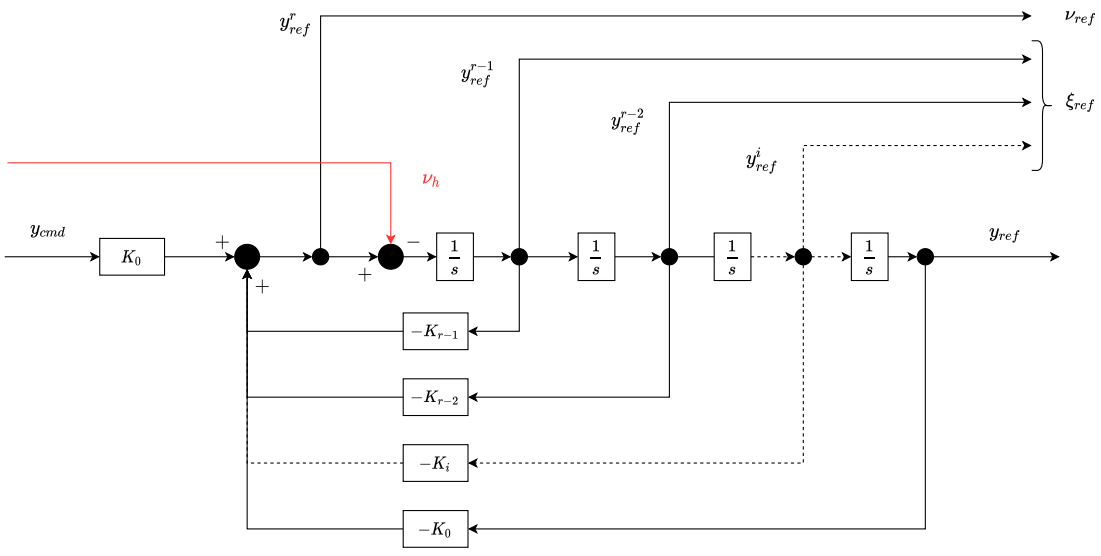

Figure 5.2: Reference model with PCH compensation [5]

5.3.2. INDI Extension on Actuators

The alleviation for saturation provided by PCH is widely used in INDI control, but does not account for actuator dynamics. A better compensation could be achieved if a model of the actuator would be included in the generation of the control increment.

A recent study [21] proposes an extended version of the INDI controller which takes into account control actuator dynamics. The effectiveness is then not considering only the effect of the actuators, but also their ”speed”. The derivation of the extended INDI starts from the expression of a non-dimensional system such as Equation 3.1. Assuming that the relative degree of the system is 1, the expression of the pseudo control input is

$$\dot{\boldsymbol{y}} = \boldsymbol{f}(\boldsymbol{x}, \boldsymbol{u}) \tag{5.9}$$

In conventional INDI, Equation 5.9 is approximated by means of Taylor series approximation. Instead, the true derivative is applied, resulting in

$$\begin{aligned}
\ddot{\boldsymbol{y}} &= \frac{\partial \boldsymbol{f}(\boldsymbol{x}, \boldsymbol{u})}{\partial \boldsymbol{x}} \cdot \dot{\boldsymbol{x}} + \frac{\partial \boldsymbol{f}(\boldsymbol{x}, \boldsymbol{u})}{\partial \boldsymbol{u}} \cdot \dot{\boldsymbol{u}} \\
\ddot{\boldsymbol{y}} &= \boldsymbol{A_e} \cdot \dot{\boldsymbol{x}} + \boldsymbol{B_e} \cdot \dot{\boldsymbol{u}} \\
\ddot{\boldsymbol{y}} &= \boldsymbol{B_e} \cdot \dot{\boldsymbol{u}} + \boldsymbol{d_{\dot{x}}} \\
\ddot{\boldsymbol{y}} &\simeq \boldsymbol{B_e} \cdot \dot{\boldsymbol{u}}
\end{aligned} \tag{5.10}$$

$\ddot{\boldsymbol{y}}$ therefore becomes the new pseudo control input $\boldsymbol{\nu}$ so that

$$\boldsymbol{\nu} \simeq \boldsymbol{B_e} \cdot \dot{\boldsymbol{u}} \tag{5.11}$$

which represents the inversion law of the extended INDI. The current law is derived such that it can be expressed in terms of the rate of change of the input, which is representative of the dynamics of the actuators. Because of this, the desired control increment can be expressed in terms of the actuator dynamics. Given a first order system representing the dynamics of the actuator used

$$\frac{u(s)}{u(s)_{cmd}} = \frac{\omega}{s + \omega}, \tag{5.12}$$

where ω represents the bandwidth of the transfer function, it can be rearranged in terms of the input increment Δu as follows

$$\begin{aligned}
u(s) &= \frac{\omega}{s + \omega} \cdot u(s)_{cmd} \\
u(s) &= \frac{\omega}{s + \omega} \cdot (\Delta u(s) + u(s)) \\
u(s) &= \frac{\omega}{s} \cdot \Delta u(s) \\
\dot{u}(s) &= \omega \cdot \Delta u(s) \\
\dot{u}(s) &= K_{act} \cdot \Delta u(s)
\end{aligned} \tag{5.13}$$

Implementing this structure in Equation 5.10 and inverting then then results in

$$\Delta \boldsymbol{u} = (\boldsymbol{B_e} \cdot \boldsymbol{K_{act}})^{-1} \cdot \boldsymbol{\nu} \tag{5.14}$$

Which provides the desired input increment by considering the actuator dynamics. If the dynamics of the pseudo control input are known and, for example, can be modeled as a first order system as in Equation 5.12, the incremental inversion law can be expressed as

$$\Delta \boldsymbol{u} = (\boldsymbol{B_e} \cdot \boldsymbol{K_{act}})^{-1} \cdot \boldsymbol{K_\nu} \cdot \Delta \dot{\boldsymbol{y}} \tag{5.15}$$

This arrangement has been presented as a viable solution to implement actuators in the open loop of the INDI controller. The technique used here provides information on the ”speed” of the actuator in the

effectiveness matrix of the controller. From Equation 5.13 it can be seen that the faster the actuator, the higher its resulting effectiveness will be compared to slower ones, which will be allocated less.

The method is therefore promising in the case of different actuators with different dynamics are combined in the same airframe. This weighted allocation of the effectiveness is however carried over after the computation of the pseudo control input, which does not contain information about what is achievable by the vehicle. If the actuator ”speed” is not considered in the reference trajectory computation, carried over by the reference model, unfeasible trajectories might still be computed. This flaw suggests that actuator compensation should be considered further in the reference model as well.

5.4. Reference Model Extension Through Vehicle Knowledge

The generation of a feasible pseudo control input trajectory for dynamic inversion is carried over by reference models (see Section 3.2). Commonly, they consist of linear models that use a set of coefficients which represent the physical limitations of the vehicle, such as in Figure 3.2. The use of a linear model does not take into account the inherent nonlinear characteristics of the vehicle, forcing it to a linear transient behavior. This can be especially a problem for vehicles with multiple flight phases, as a linear reference model would not vary with flight phase, which may result in the generation of incompatible commands in the inversion law. In addition, feeding trajectories generated by a non-varying, linear reference model would lead to a controller unable to exploit the full potential of the system. If heavy nonlinearities are expected during vehicle operation, it is fundamental that the reference model takes them into account.

5.4.1. Integrated Reference Model for Multi-Phase Vehicle

As previously mentioned in Section 4.4, the linear reference model does not take into account vehicle nonlinearities in trajectory generation. As a consequence, a change in flight phase is also not well represented. The straightforward solution for this case would be the use of a different controller for any flight phase, with the appropriate set of pseudo control inputs and suitable control allocation. Following this procedure increases however design time and complexity, reminding of a classical PID controller scheduling procedure.

As a solution to such issue, a modular reference model for the generation of global pseudo control inputs was proposed by [5]. The same set of pseudo control commands is generated for any flight phase in the flight operational envelope, allowing the need of only one single controller.

Because of the disadvantages of using the same pseudo control input for different flight phases, explained in Section 5.2, virtual control inputs (VCI) are selected for compensation. The integration of VCI in the reference model is made possible by splitting it in two separated loops.

To illustrate the functioning and logic of such controller, the same example of the transitioning VTOL UAV mentioned in Section 5.2 is considered.

The core commands for the UAV are the linear velocities in the earth frame $\dot{x}$ and the heading rate $\dot{\Psi}$

$$\boldsymbol{y}_{ref} = \begin{bmatrix} \dot{\boldsymbol{x}} \\ \dot{\boldsymbol{\Psi}} \end{bmatrix}_{cmd} \tag{5.16}$$

and pseudo control output vector as in Equation 5.3. The VCI vector consists in

$$\boldsymbol{y}_{v_{cmd}} = \begin{bmatrix} \dot{\boldsymbol{\Phi}} \\ \dot{\boldsymbol{\Theta}} \end{bmatrix}_{cmd} \tag{5.17}$$

where $\boldsymbol{\Phi}_{cmd}$ is the bank command and $\boldsymbol{\Theta}_{cmd}$ is the pitch command (see Section 5.2).

The high level structure of the integrated reference model can be then regarded as follows. The commanded derivative $\dot{\boldsymbol{y}}_{cmd}$ is estimated through a linear error controller (as in Section 3.3) based on the reference states $\boldsymbol{x}_{ref}$ generated by the outer loop reference model. The outer loop also computes the

load factor and velocities as pseudo control input and external reference states, respectively. The inner loop provides the desired body angular accelerations for the pseudo control input vector, together with Euler angles and its derivatives as external reference states. The virtual control inputs are fed to the inner loop which allow the reference model to compensate for the transient error mentioned in Section 5.2. Figure 5.3 illustrates the high level scheme.

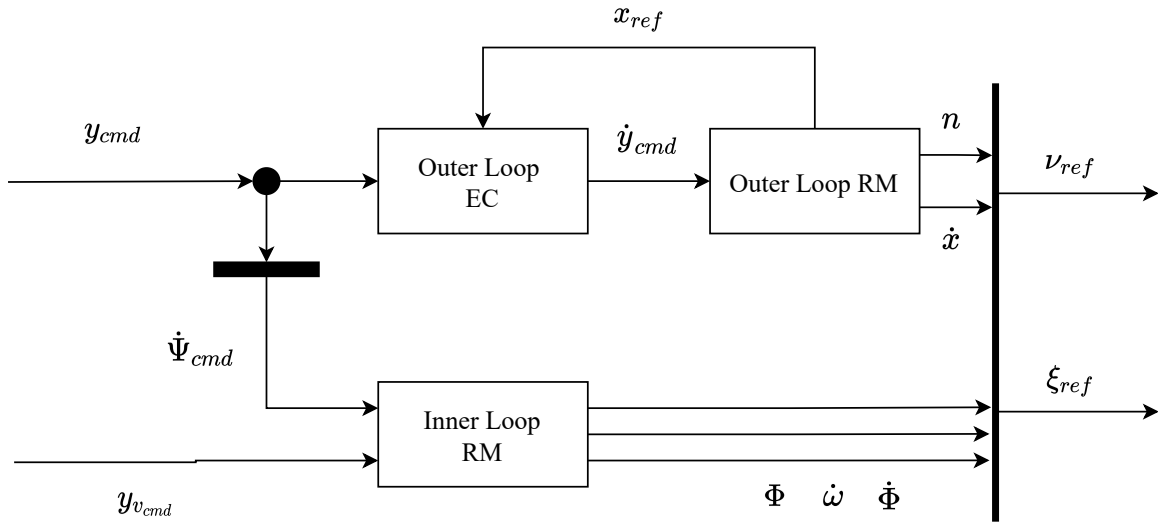

Figure 5.3: High level structure of the integrated reference model proposed by [5]

Both the outer loop and the inner loop are model based and are structured in a similar fashion. For brevity, only the structure of the outer loop is presented. The outer loop contains the reference plant dynamics and inversion laws, as illustrated in Figure 5.4, a model of the reference plant dynamics is used to estimate the reference state term x_{ref} used in the error controller and the inversion block. The load factor n is computed through nonlinear dynamic inversion (NDI).

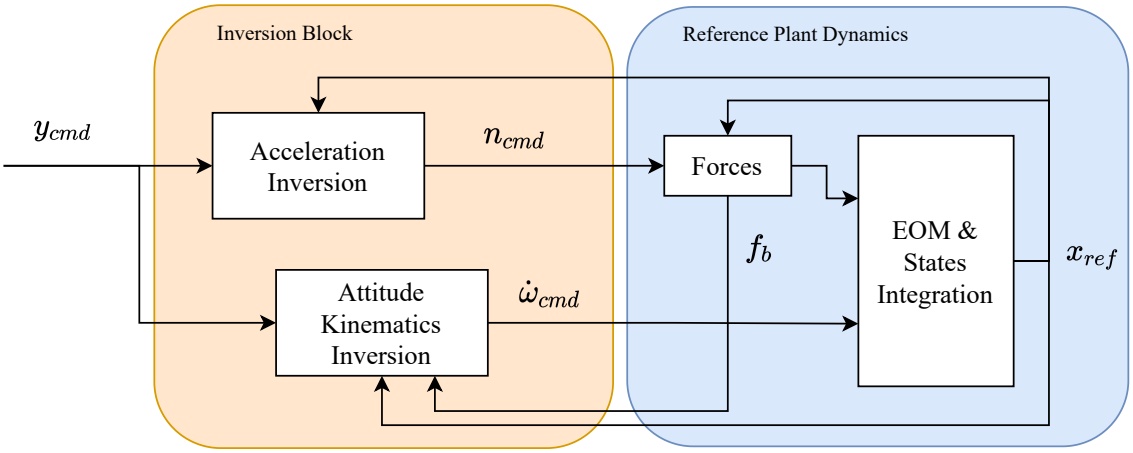

Figure 5.4: Outer loop structure of the integrated reference model proposed by [5]

By means of virtual control input and NDI in the reference model it is possible to provide a trajectory reference that takes into consideration the change of dynamics due to flight phase transition. With a linear reference model, as previously mentioned, this would not be possible, as information on the vehicle dynamics are not provided. However, results published by [5] show that the interaction between propulsive forces and aerodynamic forces cannot be described with a simplified set of equations of motion during transition maneuvers.

5.4.2. Higher Order Reference Model

Previous works on plant based reference models attempted to generate a trajectory for the INDI controller that considered the nonlinearities of the vehicle. This methods provided a more suitable set of pseudo control inputs, but these were fed to an INDI controller that neglected the state dependent increment term Δ_x (see Equation 3.2). Therefore, the state dependent term is not taken into account in these methods. As mentioned in Section 4.3, slower systems or more agile maneuvering would require compensation for such term. This includes transition scenarios where the model is subjected to high nonlinearities and aggressive accelerations. Indeed, the solution proposed in Section 5.4.1 lacked in the transition phase.

An effort to consider the effect of the state dependent increment by preserving the model-free robustness of INDI was made by [4]. In this approach, plant knowledge is used for the generation of a feedforward term one derivative level higher than the pseudo control input, and therefore the relative degree of the system. The approach is applied to an extended INDI controller proposed by [21], which takes into consideration first and second order actuators, in the fashion explained in Section 5.3.2.

[4] considers the continuous extension inversion law of INDI

$$\dot{\boldsymbol{u}}_{cmd} = \boldsymbol{B}_{\nu}^{-1} \cdot \dot{\boldsymbol{\nu}}_{u,cmd}, \tag{5.18}$$

and shows that if substituted in the transformed system mentioned in Equation 5.9 as follows

$$\dot{\boldsymbol{\nu}} = \boldsymbol{A_e} \cdot \dot{\boldsymbol{x}} + \boldsymbol{B_e} \cdot \boldsymbol{B_e}^{-1} \cdot \dot{\boldsymbol{\nu}}_{u,cmd} \tag{5.19}$$

A state dependent term Δ_x exists such that

$$\dot{\boldsymbol{\nu}} - \dot{\boldsymbol{\nu}}_{u,cmd} = \boldsymbol{A_e} \cdot \dot{\boldsymbol{x}} = \Delta_x \tag{5.20}$$

Usually, an error controller such as in Section 3.3 is used as compensation for this, but usually it is linear (see Figure 3.3) and does not suggest corrections based on the nonlinearities of the vehicle model.

This limitation is tackled in [4] by using a reference plant model of type

$$\boldsymbol{\nu}_R = \boldsymbol{F}_R(\boldsymbol{x}_R, \boldsymbol{u}_R) \tag{5.21}$$

which is continuously extended as in [21], leading to affinity between the control input derivative and the pseudo control input derivative

$$\dot{\boldsymbol{\nu}}_R = \frac{\partial \boldsymbol{F}_R}{\partial \boldsymbol{x}_R} \cdot \dot{\boldsymbol{x}}_R + \frac{\partial \boldsymbol{F}_R}{\partial \boldsymbol{u}_R} \cdot \dot{\boldsymbol{u}}_R = \boldsymbol{A}_R \cdot \dot{\boldsymbol{x}}_R + \boldsymbol{B}_R \cdot \dot{\boldsymbol{u}}_R \tag{5.22}$$

An internal reference model (such as in Figure 3.2) is employed to obtain the internal reference pseudo control rate command $\dot{\boldsymbol{\nu}}_{iR,cmd}$. From this and from Equation 5.22, the input command rate can be derived through inversion

$$\dot{\boldsymbol{u}}_R = \boldsymbol{B}_R^{-1} \cdot (\dot{\boldsymbol{\nu}}_{iR,cmd} - \underbrace{\boldsymbol{A}_R \cdot \dot{\boldsymbol{x}}_R}_{\dot{\boldsymbol{\nu}}_{x,R}}) \tag{5.23}$$

with $\boldsymbol{A}_R \cdot \dot{\boldsymbol{x}}_R$ being the state dependent term $\dot{\boldsymbol{\nu}}_{x,R}$ usually neglected. This time however is computed through the reference plant in Equation 5.21, and fed back to internal reference command for generation of the feedforward control input rate $\dot{\boldsymbol{\nu}}_{ff}$, which is finally able to deliver model based commands to the INDI controller. The reference plant dynamics then become

$$\begin{aligned}\dot{\boldsymbol{\nu}}_R &= \boldsymbol{A}_R \cdot \dot{\boldsymbol{x}}_R + \boldsymbol{B}_R \cdot \boldsymbol{B}_R^{-1} \cdot (\dot{\boldsymbol{\nu}}_{iR,cmd} - \boldsymbol{A}_R \cdot \dot{\boldsymbol{x}}_R) \\ \dot{\boldsymbol{\nu}}_R &= \underbrace{\boldsymbol{A}_R \cdot \dot{\boldsymbol{x}}_R}_{\dot{\boldsymbol{\nu}}_{x,R}} + \underbrace{(\dot{\boldsymbol{\nu}}_{iR,cmd} - \boldsymbol{A}_R \cdot \dot{\boldsymbol{x}}_R)}_{\dot{\boldsymbol{\nu}}_{ff}}\end{aligned} \tag{5.24}$$

Which does not only show that $\dot{\boldsymbol{\nu}}_R = \dot{\boldsymbol{\nu}}_{iR,cmd}$, but proves that the reference model does not need the effectiveness matrix $\boldsymbol{B}_R$ for the estimation of the feedforward term. For state term compensation, the additional knowledge required by the higher order reference model is therefore concerning $\boldsymbol{A}_R$ only. If control actuator dynamics are considered, $\dot{\boldsymbol{\nu}}_{iR,cmd}$ should also contain compensation from an error controller, as contributions outside the plant dynamics create a deviation from the reference trajectory of the internal reference model. This whole extension is visually represented in Figure 5.5.

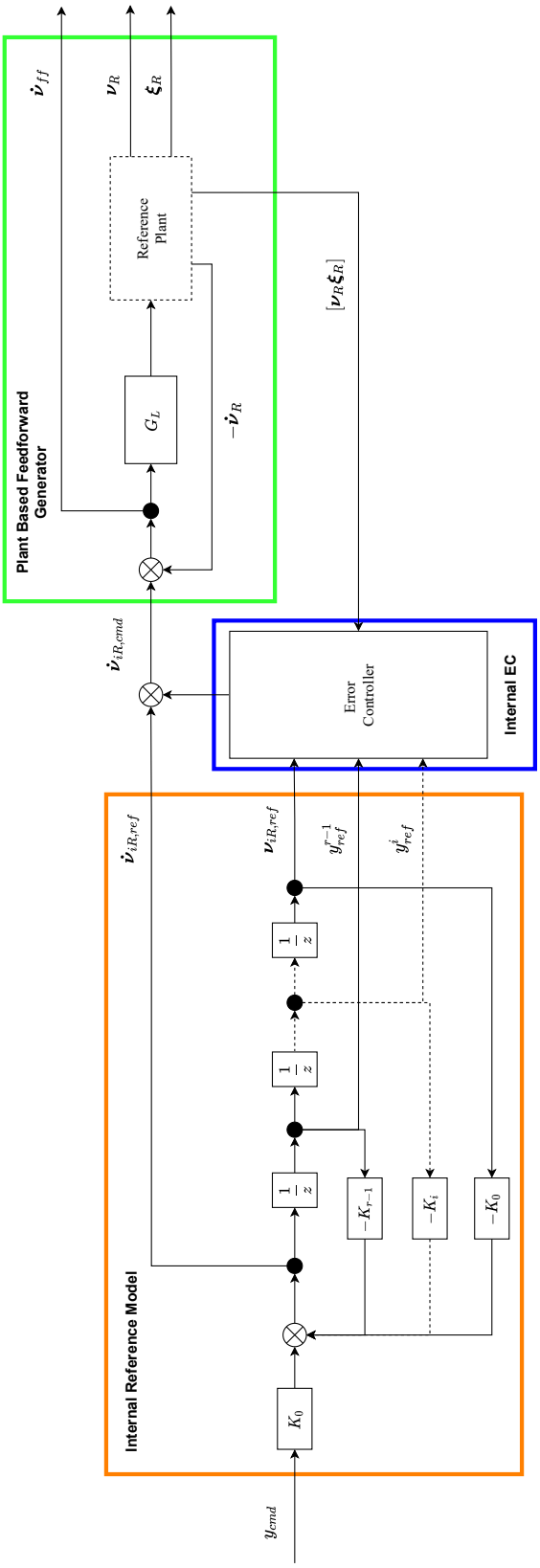

Figure 5.5: Higher Order Reference Model structure as described in [4]

6

Assessment of Existing Solutions

The methods and techniques reported in Chapter 5 can form a solid base for the design of a controller solution that can consider actuator and vehicle dynamics to enhance trajectory tracking performance and robustness.

In order to have a better understanding of qualities and the potential of existing solutions, it could be insightful to assess these by using a common tool. In this way, the relative impact of a set of improvements can be clearly exposed, together with its limitations.

The coming chapter therefore attempts to give a clear overview of what is more methods are more promising and what should be discarded, based on simple simulation conducted on a common model.

6.1. Model Adopted for Comparison

The ideal common vehicle that should be used for such a preliminary comparison is easy to implement, simple to understand, and provides the necessary traits which allow for a straightforward application of the considered solutions.

Based on such, a non-linear F-16 simulation tool running on Matlab is selected[1]. The aerodynamic model of the aircraft is derived from [18]. The tool allows for linearization of the nonlinear model around a trim condition. The output of the linearization are three state space system: full, lateral and longitudinal.

For this assessment, the model is linearized around a cruising phase condition at a true airspeed V_t of 700 ft/sec and an altitude h of 10000 ft. Once the linearization is completed, the longitudinal state space system is considered. From this, the short period model is extrapolated, resulting in the state space system in

$$\begin{bmatrix} \dot{\alpha} \\ \dot{q} \end{bmatrix} = \begin{bmatrix} C_{Z_\alpha} & C_{Z_q} \\ C_{m_\alpha} & C_{m_q} \end{bmatrix} \cdot \begin{bmatrix} \alpha \\ q \end{bmatrix} + \begin{bmatrix} C_{Z_{\delta_e}} \\ C_{m_{\delta_e}} \end{bmatrix} \cdot \delta_e \tag{6.1}$$

For short period motions, it is also safe to assume that C_{Z_q} is unity and $C_{Z_{\delta_e}} = 0$. These assumptions further simplify the model, leading to the equations of motion in Equation 6.2 below.

$$\begin{aligned} \dot{\alpha} &= C_{Z_\alpha} \cdot \alpha + q \\ \dot{q} &= C_{m_\alpha} \cdot \alpha + C_{m_q} \cdot q + C_{m_{\delta_e}} \cdot \delta_e \end{aligned} \tag{6.2}$$

Since the idea is to implement actuator dynamics into INDI, among other things, a model of the elevator must be made available. For simplicity, the elevator dynamics are modeled as a first order system.

[1] https://dept.aem.umn.edu/people/faculty/balas/darpa_sec/SEC.Software.html

$$\frac{\delta_e}{u} = \frac{\omega}{\omega + s} \tag{6.3}$$

where $\omega \div 0$. The system presented is used to compare and assess different methodologies explored in this literature study. The comparison is performed by looking at the change in tracking performance of a desired pitch rate trajectory, with disturbances.

During the assessment it is sometimes easier but still fairly representative, to use a simplified version of the short period motion in Equation 6.2, which does not consider the dynamics of the angle of attack α. The system can be then simply described as

$$\dot{q} = C_{m_q} \cdot q + C_{m_{\delta_e}} \cdot \delta_e \tag{6.4}$$

The vehicle (a fighter aircraft) and the motion selected allow for the design of a SISO INDI controller, a reference model and a linear error controller, which brings into practice the structure of Figure 3.4. This starting point allows then to test the claims from a wide subset of solutions exposed in Chapter 5. Unfortunately, solutions for flight phase transition improvements or MIMO applications are not applicable on this test simulation. These are planned to be implemented on simulations of more complex vehicles, subsequent to the termination of this report.

6.2. Actuator Consideration on INDI Inversion Law

Given the system in Equation 6.2, the conventional INDI control law can be easily derived. For tracking of the pitch rate q, assuming an ideal actuator and neglecting the state dependent terms, the incremental inversion law becomes

$$u = \frac{1}{C_{m_{\delta_e}}} \cdot (\dot{q}_{ref} - \dot{q}) + \delta_e \tag{6.5}$$

which can be easily implemented for trajectory tracking. It is however always the case, in reality, that the vehicle has actuators with non-instantaneous dynamics, such as in Equation 6.3. Assuming the actuator to be infinitely fast can, in certain cases (e.g. while employing a servo actuator), cause performance degradation and poor disturbance rejection, as visible in Figure 6.1. Here a trajectory for the pitch rate q_{ref} is provided in blue. To obtain $\dot{q}_{ref}$, a gain of 10 is used. This signal is fed to the INDI control law as in Equation 6.5. The control input signal u is then used to control a plant with an instantaneous elevator (i.e. $\tau_{el} = 0s$), in yellow, and one with a first order elevator with time constant $\tau_{el} = 0.1s$, in red. For the first case, the elevator command δ_e is fed with a delay of z^{-1}. An external disturbance is introduced at time $t = 7s$.

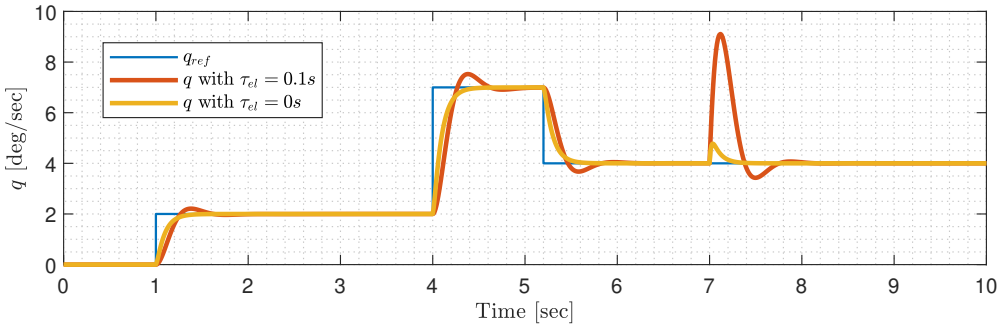

Figure 6.1: Tracking and robustness degradation due to unconsidered actuator dynamics

The more relevant compensation attempt for actuators dynamics can be done in line with the reasoning exposed in Section 5.3.2. In a case where the pitch rate q is to be controlled, the expression for the pitch acceleration $\dot{q}$ (from Equation 6.2) is differentiated, resulting in the extended control law

$$\begin{aligned} \ddot{q} &= C_{m_\alpha} \cdot \dot{\alpha} + C_{m_q} \cdot \dot{q} + C_{m_{\delta_e}} \cdot \dot{\delta}_e \\ \ddot{q} &\simeq C_{m_{\delta_e}} \cdot \dot{\delta}_e, \end{aligned} \tag{6.6}$$

which, on the basis of Equation 5.13, can be expressed as

$$\ddot{q} = C_{m_{\delta_e}} \cdot \omega \cdot (u - \delta_e) = C_{m_{\delta_e}} \cdot \omega \cdot \Delta u \tag{6.7}$$

Equation 6.7 can be inverted to provide an INDI law that considers actuator dynamics and compensates for that

$$\Delta u = \frac{1}{C_{m_{\delta_e}} \omega} \cdot \ddot{q}_{des} \tag{6.8}$$

where $\ddot{q}_{des}$ represents the desired pitch jerk to be tracked, which can be obtained from a linear reference model and and error controller compensation, as in

$$\ddot{q}_{des} = \underbrace{\omega_e \cdot (\dot{q}_{des} - \dot{q})}_{EC} + \underbrace{\ddot{q}_{ref}}_{RM} \tag{6.9}$$

Where ω_e is a gain value selected to meet the desired dynamics of the error controller. Such a structure and adaptation improves the overall tracking accuracy by reducing model mismatch and by providing a more efficient response to disturbances, as visible in Figure 6.2, which compares the tracking accuracy already presented in Figure 6.1 with the tracking accuracy achieved with the extended control law from Section 5.3.2.

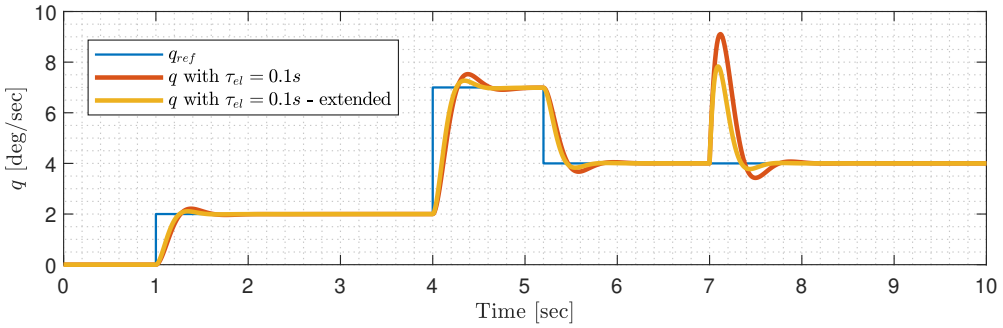

Figure 6.2: Tracking and robustness improvement due to actuator compensation

It has to be pointed out however that the reference model is providing a trajectory command that is not based on the real dynamics of the vehicle, but is linear. The compensation is therefore being applied on a trajectory that does not exploit all the characteristics of the plant. The same applies to disturbances.

6.3. State Increment Compensation for Feedforward Generation

The method proposed by [4] provides a good strategy to include actuator dynamics in the INDI loop and take into account the state increment term without compromising the inherent robustness of INDI. In addition, it enables tracking of higher order derivatives of the pseudo control input, which is ideal for improving performance during agile maneuvering. In addition, perfect tracking is only achievable in cases where no external disturbances are present and the first derivative of the pseudo control input can be expressed in terms of the pseudo control input only.

In the case for the short period, for example, the derivative of the angle of attack α should be available for the computation of the feedforward term. Given the fact that the pseudo control input vector $\boldsymbol{\nu}$ contains only the pitch rate q, and the reference model only generates a trajectory for $\boldsymbol{\nu}$, as it conventionally does

(see Section 3.2), α is not available. In addition, an external disturbance, and the consequent deviation from the trajectory, is not fed back to the internal error controller in Figure 5.5, which is only responsible for compensating sensor dynamics or other discrepancies in the open loop. The only section which then can compensate disturbances is the external error controller. This results in a linear disturbance compensation which does not account for the complex nonlinearities of the vehicle.

Both limitations have a degrading impact on the trajectory tracking performance of the platform. If the short period model of [4] is considered, the angle of attack can be ignored, as its dynamics consist of simply

$$\dot{q} = C_{m_q} \cdot q + C_{m_{\delta_e}} \cdot \delta_e \tag{6.10}$$

If the state term compensation method presented in Figure 5.5 is considered, the final inversion law based on such dynamics would track a pitch jerk $\dddot{q}_{des}$ from Equation 6.9 which also contains state dependent terms, resulting in

$$\Delta u = \frac{1}{C_{m_{\delta_e}}\omega} \cdot \ddot{q}_{des} = \frac{1}{C_{m_{\delta_e}}\omega} \cdot (\omega_e \cdot (\dot{q}_{des} - \dot{q}) + \ddot{q}_{ref} - C_{m_q} \cdot \dot{q}_{ref}) \tag{6.11}$$

In this particular case, the feedforward term is only in terms of the internal reference model trajectory and its higher order derivatives. This makes the derivation by [4] achievable. However, if the real plant contains also the dynamics of the angle of attack as in Equation 6.2, Equation 6.11 should also include it, leading to an inversion law which requires the knowledge of the dynamics of α

$$\Delta u = \frac{1}{C_{m_{\delta_e}}\omega} \cdot \ddot{q}_{des} = \frac{1}{C_{m_{\delta_e}}\omega} \cdot (\omega_e \cdot (\dot{q}_{des} - \dot{q}) + \ddot{q}_{ref} - C_{m_q} \cdot \dot{q}_{ref} - C_{m_\alpha} \cdot \dot{\alpha}_{ref}) \tag{6.12}$$

From Equation 6.2, this can be further extended to

$$\Delta u = \frac{1}{C_{m_{\delta_e}}\omega} \cdot \ddot{q}_{des} = \frac{1}{C_{m_{\delta_e}}\omega} \cdot (\omega_e \cdot (\dot{q}_{des} - \dot{q}) + \ddot{q}_{ref} - C_{m_q} \cdot \dot{q}_{ref} - C_{m_\alpha} \cdot q_{ref} - C_{m_\alpha} \cdot C_{Z_\alpha} \alpha_{ref}) \tag{6.13}$$

Which raises a question regarding what should provide the value for α_{ref}. Should the reference model provide that? Or can the state estimation of the vehicle feedback this value? It is important to solve this issue properly, because if a proper state dependent compensation is not conducted for the system in Equation 6.2, the tracking degrades, as shown in Figure 6.3: here two different plants, one containing the dynamics of α and the other not, are compensated only with what is directly available from the internal reference model, meaning the pitch acceleration $\dot{q}$ only. A compensation for the angle of attack is therefore not applied for the full plant; the trajectory tracking clearly degrades. Also note how the tracking performance worsens in segments where higher accelerations are required (see $t = 4s$); this is well in line with what stated in Section 4.3 regarding agile maneuvering. Also, a note should be made on how the disturbance rejection performance at $t = 7s$ remains unvaried (further discussion on this matter in the following sections). The coming subsection speculates on several ways to solve this issue.

6.3.1. Full Plant Dynamics Inclusion in Reference Model

Real dynamics present, almost always, an interrelation between the different states that describe the motion of the vehicle considered. Usually, there are more states affecting the plant than in the desired trajectory. This is the case for the example discussed in this chapter: the provided trajectory enables tracking of the pitch rate q and its derivatives, but not α, which however also affects q, as is clear from Equation 6.13.

Ideally, a trajectory should be provided for α as well, generating a α_{ref} signal which can be fed for feedforward compensation. However, the idea of this research is to keep the simplicity of INDI and allow tracking with a low amount of information. The signal α must therefore be generated in a different

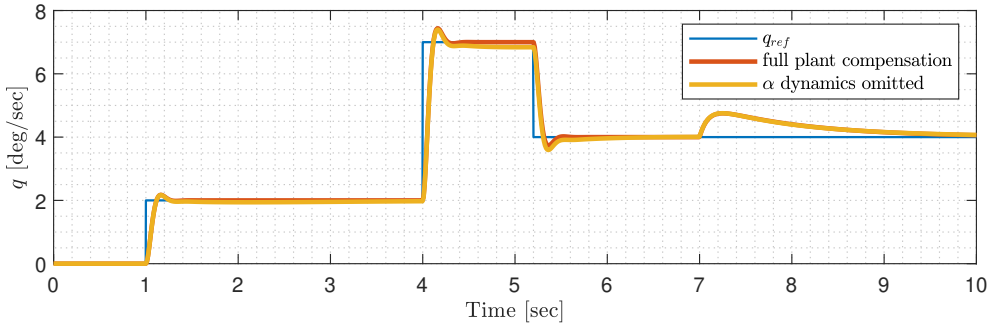

Figure 6.3: Tracking performance degradation due to state dynamics omission in compensation

way. Based on the literature gathered, the two main methods that can be used to achieve this are mainly two:

- **Plant State Feedback**: The states which affect the feedforward generation but are not part of the reference trajectory are directly taken from the vehicle actual state and measured.
- **Differential Flatness**: The state dependent term is expressed in terms of the reference trajectory and its derivatives only through differential flatness transform.

The following paragraphs show their implementation and compare the two methods.

State Feedback

The inversion law in Equation 6.8 usually sees $\ddot{q}_{des}$ as the reference trajectory generated by a linear reference model. In the method from [4], the state dependent part $\ddot{q}_{R,x}$ of this pseudo control input (which represents the vehicle dynamics in function of the state) is subtracted, leaving $\ddot{q}_{R,u}$ as final feedforward (see also Equation 5.24)

$$\ddot{q}_{des} = \ddot{q}_R - \ddot{q}_{R,x} = \ddot{q}_{R,u} \tag{6.14}$$

leading to an inversion law in terms of $\ddot{q}_{R,x}$

$$\Delta u = \frac{1}{C_{m_{\delta_e}}\omega} \cdot (\ddot{q}_R - \ddot{q}_{R,x}) \tag{6.15}$$

The term $\ddot{q}_{R,x}$, as previously stated regarding the full short period model in Equation 6.13, contains α, which is not directly provided by the internal reference model. Assuming that no external disturbances affect the state, and that the state dependent compensation is perfect (therefore no model uncertainty), α can be obtained from the direct measurement of the state. This is also true for q, since it is true that $q_R = q$.

Differential Flatness

In Section 5.1 the differential flatness transform method is presented. The main advantage of differential flatness is that, if the system considered is flat with respect to its flat output, each one of its states can be expressed in terms of the selected flat output and its derivatives. The process of expressing one of the states or the inputs in this form is referred as differential flatness transform.

The application of this technique could benefit the expression for the inversion law in Equation 6.13, as it could lead to an expression of α_{ref} in terms of q_{ref} and its derivatives. If this is achieved, the full plant dynamics can be expressed only in terms of the provided trajectory and the input, retaining the simplicity of use and providing higher accuracy in tracking.

It can be proven that the inversion law for the full short period motion can be transformed with differential flatness. Starting from Equation 6.2, the equation for the change in pitch rate $\dot{q}$ can be further differentiated in

$$\ddot{q} = C_{m_\alpha} \cdot \dot{\alpha} + C_{m_q} \cdot \dot{q} + C_{m_{\delta_e}} \cdot \dot{\delta}_e \tag{6.16}$$

$\dot{\alpha}$ can be substituted with the dynamics of the angle of attack. The same holds for $\dot{\delta}_e$, leading to

$$\ddot{q} = C_{m_\alpha} C_{Z_\alpha} \cdot \alpha + C_{m_\alpha} \cdot q + C_{m_q} \cdot \dot{q} + C_{m_{\delta_e}} \omega_e \cdot (u - \delta_e) \tag{6.17}$$

α can be expressed in terms of the input and the flat output by rearranging the equation for the pitch dynamics in Equation 6.2. The outcome results in

$$\ddot{q} = C_{m_\alpha} C_{Z_\alpha} \cdot \left(\frac{\dot{q} - C_{m_q} \cdot q - C_{m_{\delta_e}} \cdot \delta_e}{C_{m_\alpha}} \right) + C_{m_\alpha} \cdot q + C_{m_q} \cdot \dot{q} + C_{m_{\delta_e}} \omega_e \cdot (u - \delta_e) \tag{6.18}$$

which can be rearranged in the form proposed in Equation 6.11

$$u - \left(\frac{C_{Z_\alpha}}{\omega} + 1 \right) \cdot \delta_e = \frac{1}{C_{m_{\delta_e}} \omega} \cdot \left(\ddot{q} - \left(C_{Z_\alpha} + C_{m_q} \right) \dot{q} + \left(C_{m_q} C_{Z_\alpha} - C_{m_\alpha} \right) q \right) \tag{6.19}$$

The incremental function is now full expressed in terms of the desired trajectory for q and its derivatives.

Comparison on Performance
For a scenario with no disturbances and perfect representation of the model, both methods allow for a perfect tracking of the trajectory generated by the internal reference model, as visible from Figure 6.4. This of course is not enough to determine in which direction the extension should go yet, as the effect of model mismatch and external disturbances are not taken into account. The following work investigates such limitations.

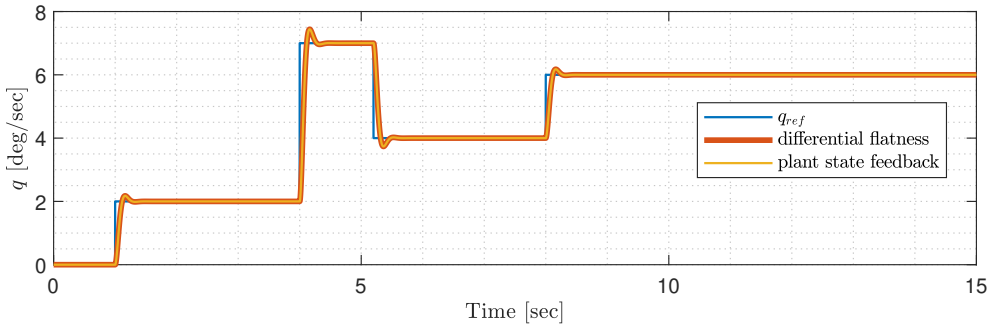

Figure 6.4: Perfect reference trajectory tracking through both differential flatness and plant state compensation methods

6.3.2. Assessment on State Feedback Compensation Method

The method used for state compensation on the feedforward term, proposed by [4], aims to generate the state compensation term by using the output of the reference model. As already mentioned in Section 6.3.1, the state dependent term $\dot{\nu}_{x,R}$ (from Equation 5.24) can depend on states that are not contained in the reference model. It has been shown in Figure 6.4 that the missing states (as well as all the states) can be obtained from the plant's state estimation pipeline. It is not yet known however what happens when these states are polluted by external disturbances or the model used for the compensation does not exactly match the plant model. This information is not available in the literature and this section only provides a high level assessment of what the possible effects can be and how the investigation should proceed in the work consequent to this literature study.

Looking back to Equation 6.8, $\ddot{q}_{des}$ can be expressed for the model in Equation 6.2 as

$$\ddot{q}_{des} = \ddot{q}_{ref} - C_{m_q} \cdot \dot{q}_{ref} - C_{m_\alpha} \cdot \dot{\alpha}_{ref} \tag{6.20}$$

This follows from Figure 5.5, where both $\dot{q}$ and $\dot{\alpha}$ are provided by the reference model, therefore the subscript ref. Assuming that these are not available by the reference model, $\ddot{q}_{des}$ may then take these values from the state estimation of the vehicle, resulting in

$$\ddot{q}_{des} = \ddot{q}_{ref} - C_{m_q} \cdot \dot{q} - C_{m_\alpha} \cdot \dot{\alpha} \tag{6.21}$$

Without disturbances and perfect model knowledge Equation 6.20 and Equation 6.21 are the same during the whole tracking. One of the questions now is what happens as soon as an external disturbance is introduced. It has been shown in Figure 6.3 that the disturbance rejection is not influenced by whether or not the state term compensation is present or not. This means that the method from [4] has no affect on the disturbance response, but its variation from Equation 6.21 has. From simulations ran on the F16 short period model from Equation 6.2, it has been found that feeding back the plant states to the state term compensator, rather than the reference states, introduces a better predictability of the disturbance response.

This can be visually represented by Figure 6.5. Here, four different disturbance responses are overlapped. Firstly, the plant of Section 6.1 is considered (with the same flight phase), with both $\dot{q}$ and $\dot{\alpha}$ fed back for state term compensation and without. Secondly, the same pair is used, but this time the coefficients that represent the model in the state compensation, namely C_{m_q} and C_{m_α}, are varied (multiplication by -2). As clear from the overlapping, a change in the plant dynamics affects the disturbance response for a simple INDI controller, but not for the higher order reference model method with plant state feedback.

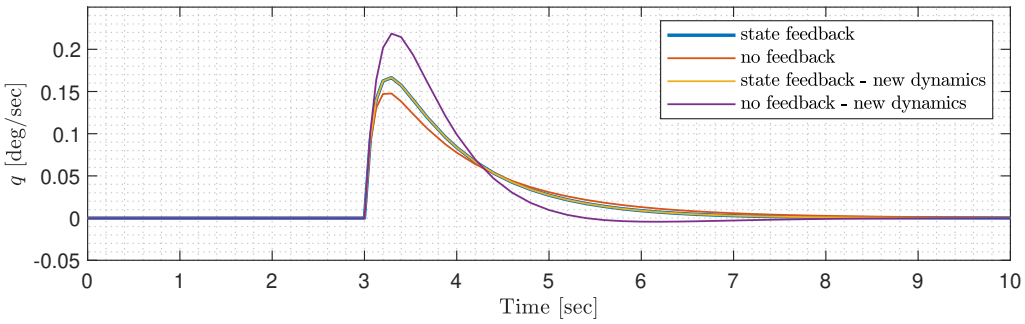

Figure 6.5: Steady state error due to differential flatness based state term compensation

This behavior is interesting for real life applications as it ensures that, if the model dynamics are known, the disturbance rejection behavior is always the same. This is particularly useful for highly nonlinear vehicles with deep changes in motion dynamics between different flight phases. Instead of designing different error controllers and a switching logic to keep a constant and predictable disturbance rejections, this method could potentially remove this need.

For the coming work, some attention should also be directed towards the effect of feeding back the state instead of the reference model when the model is not matching perfectly with the dynamics of the plant. To investigate differences, the same plant used in the disturbance investigation above is considered, with the same state compensation method. Each pair has one controller with both $\dot{q}$ and $\dot{\alpha}$ fed back for state term compensation and the other one only α, while $\dot{q}_{ref}$ is taken from the reference. One of the pairs has different C_{m_q} and C_{m_α} (multiplication by -2). All controllers have a model mismatch equal to 0.3 times the real model (the state increment compensation is therefore still useful, but not perfect). As observable from Figure 6.6, changing the state dynamics can make these more or less effective, therefore more visible when not compensated for. However, feeding back the plant state rather than the reference appears to not vary the tracking excessively.

6.3.3. Assessment on Differential Flatness Compensation Method

In an ideal scenario where the model is known perfectly and no disturbances are applied, the differential flatness approach allows for perfect internal reference trajectory tracking (see Figure 6.4). This is also

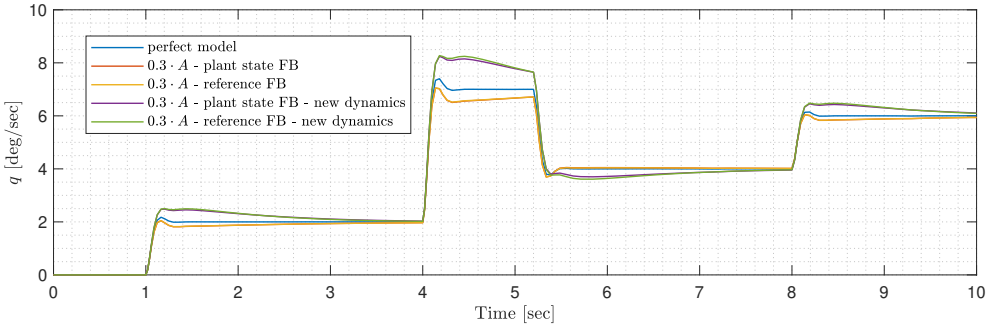

Figure 6.6: Model mismatch effect with varying plant dynamics and plant state or reference feedback

achieved by the plant state feedback method. However, by applying differential flatness transform, it is possible to use the output command (for this case, q), and its higher order derivatives, as the only information to be able to provide a full state compensation. This removes the need to consider the angle of attack α (referring to the short period case), which in practical terms translates to less sensors on board and lighter software.

The implementation of such method on the short period model of the F16, shown in Equation 6.19, presents however several issues in more realistic scenarios. As shown in Figure 6.7 below, when the model used for the compensation does not perfectly match with the plant dynamics, or disturbances are introduced ($t_{d1} = 7s$ and $t_{d2} = 9s$), the differential flatness compensation method introduces steady state errors.

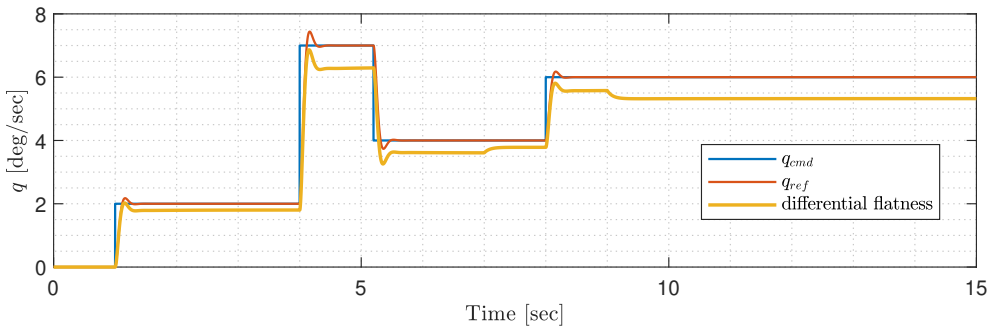

Figure 6.7: Steady state error due to differential flatness based state term compensation

A steady state error originating from a step input means that the system is missing an integrator in the open loop transfer function. For the short period example, adding an integrator would mean to track the lower order derivative of the pitch rate q_R, which corresponds to the pitch angle θ_R. This means that the error controller needs to be augmented to consider also the pitch angle error, and feed that to the feedforward term. The effect of introducing an integrator in the open loop can be seen in Figure 6.8 below.

These observations about solving the issues presented in Section 6.3.1 with differential flatness help to provide a broader understanding of what is eventually needed to be considered during the design of a large scale controller for larger, more complex systems.

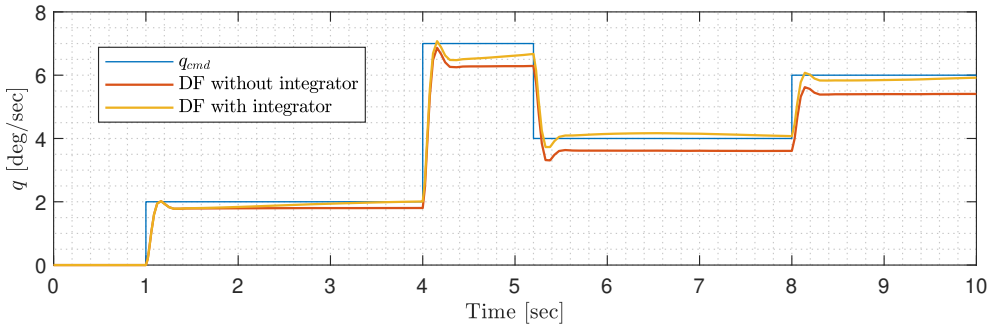

Figure 6.8: Steady state error compensation with introduction of integrator in the open loop

7

Research Plan for the Thesis Project

The material presented until now in this work provides the necessary package of information to be able to clearly identify the knowledge gap in the research field discussed: incremental nonlinear dynamic inversion control. The finding of such gap allows for the generation of a precise research strategy that aims to achieve a relevant improvement in the field of INDI control.

This conclusive chapter has therefore the role of readapting the preliminary research plan presented in Chapter 2 on the basis of the new findings of this literature study.

7.1. Knowledge Gap

At the start of this report the focus was directed towards an improvement of the main limitations that affect the INDI control strategy by means of model based solution, especially the actuators. Several flaws in the INDI pipeline were found. Consequently, given the interest that such controller aroused in the academic environment, a good amount of different compensation methods were identified. The most recent innovations were however validated in a simple simulation environment and ideal conditions. Because of this, some were put to the test with simulation based on an F16 model running on INDI.

Based on the investigation summarised above, it was found that no real life vehicle has flown with both a state term compensation and actuator compensation on its reference trajectory. Also no actuator compensation strategy is applicable today on such complex vehicles. Most importantly, it has been found that all the most promising compensation strategies identified until today provide an improvement in the trajectory tracking, but not in disturbance rejection. It can be then safely assumed that there is no solution for a model based disturbance rejection strategy for an INDI controller.

As covered in Chapter 1, drone operations are becoming increasingly complex and challenging. The need for robust outdoor solutions is present and many drone solutions proposed even by the most advanced companies have to face the constant challenge of reacting firmly to bad weather conditions. This is especially true for a certain set of vehicles with large aerodynamic surfaces, such as flying wings.

Based on the above, the knowledge gap can be then summarised in the following sentence:

To date, an INDI controller that uses model knowledge and actuator dynamics to improve the response to external disturbances and smooth tracking of the reference trajectory is missing. In addition, a validation of such controller on a wide flight envelope in real life has not been conducted.

Based on this, a solid research strategy can be developed.

7.2. Research Objective

From the knowledge gap statement, the research objective follows directly:

How can the knowledge of vehicle and actuator dynamics be used to enable robust disturbance rejection and accurate tracking while employing and INDI controller, and preserving its simple core structure.

Which will be achieved by

Using the state and model information of the vehicle to construct a reference model able to generate a trajectory that exploits the full capabilities of the platform and prioritizes disturbance compensation.

7.3. Research Questions

As a comparison with the research question stated in Chapter 2, the one to be answered in the following work is narrowed down to the disturbance rejection segment, by still retaining the importance of model-based and actuator-based solutions. In brief:

How can actuator dynamics and model knowledge improve the overall trajectory tracking performance of a vehicle controlled by means of an INDI strategy, including disturbances?

Given the relevance of such question in the practical environment as well, it is important for this research topic to be validated in an real environment, meaning with a physical test vehicle and representative maneuvers. The research question can be then decomposed in further sub-questions.

A How can the trajectory tracking accuracy of a vehicle controlled by INDI improve by including the actuator dynamics and the state dependent dynamics in the generation of the control input command?

B How can the current solutions for improved trajectory tracking be expanded to augment disturbance rejection?

C Can the flight envelope of a vehicle be expanded by this type of augmentation?

D How complicated and expensive is to obtain the state estimation required to compensate for state dependent terms?

E How much is the influence of noise affecting the compensation?

7.4. Research Strategy

To achieve the objective set in this report, a detailed plan must be laid down before the implementation of the improvements starts. During the literature study, the application spectrum has been narrowed down to identify the research gap. Now, the opposite should take place: to understand and assess fully the relevance of the research gap in a wide application environment, a scale up strategy must be carried over.

Firstly, the model of the F16 will be used further to identify a method for disturbance rejection. The validation of such improvement, together with the one on trajectory tracking improvement, is then applied to a more complex system, which resembles more a real case scenario. The system selected for this purpose consists in an over-actuated quad-plane (for more information consult Appendix A). If a good potential is perceived in the results of the simulations, the controller can then be brought to the practical world, where the final verdict can be then made. A more detailed overview of the plan can be found in the following section, where the Gantt chart is presented.

7.5. Gantt Chart

Here below, a Gantt chart is included highlighting the most important tasks and milestones required for the completion of the thesis project. For more compactness, the new controller design is addressed as SC-INDI, where SC stands for State Compensated.

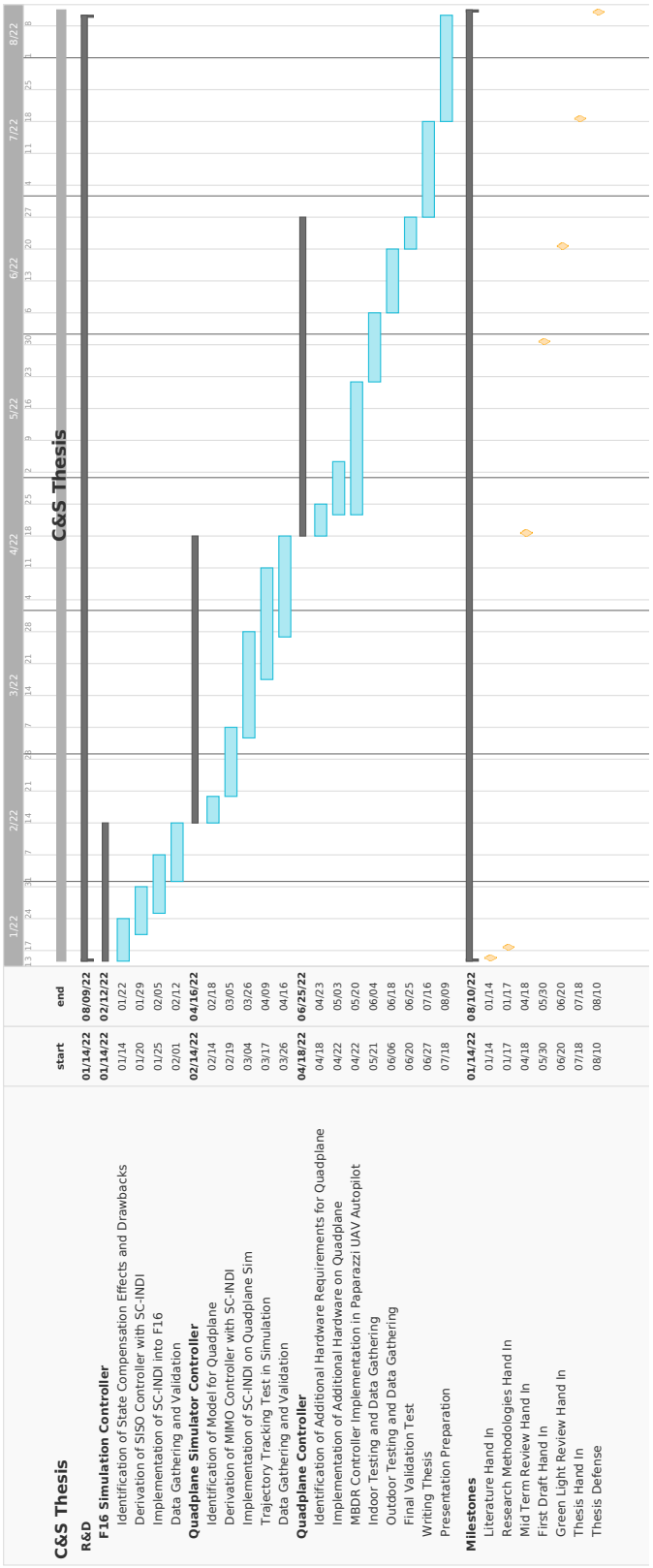

Figure 7.1: Gantt chart highlighting the required tasks and milestones for the successful completion of the Master Thesis

8

Conclusion

The work presented in this report summarises the current literature developed until this time regarding the limitations of Incremental Nonlinear Dynamic Inversion (INDI) Control and the solutions proposed so far to compensate for these. It was found that these do not yet allow an optimal performance on a wide array of vehicles and flights. A relevant topic for example concerns the consideration of actuator dynamics in the trajectory generation. These are usually neglected under the assumptions that the actuators used are fast, but this is not the case for platforms such as fixed wings or some hybrids configurations. Also the neglection of the vehicle dynamics can lead to tracking degradation in some cases, such as agile manoeuvres, where rapid changes of state are required. In addition to this, and somewhat interrelated, the performance of highly nonlinear vehicles can be limited by the linear nature of the reference model and error controllers that provide the trajectory to the INDI controller. Based on this collection of drawbacks, it can be claimed that the performance degradation is limited to complex vehicles performing agile maneuvering. However, given the direction of the industry and the increasing demand of challenging outdoor operations, the issue is highly relevant.

Based on these existing limitations, several compensation methods arose. If the inversion law of the INDI controller is considered, it has been found that this one can be expanded by avoiding the linearization and neglection of the state term by employing differential flatness for the expression of the command input. This method allows for a consideration of the nonlinearities in the command generation, but it heavily corrupts the simplicity of the inversion law and does not even consider actuator dynamics, also part of the model. However, differential flatness is a powerful method that can be applied in other segments of the controller, such as in the reference model. It has been found however that actuator dynamics can be added to the INDI inversion law by using the first order derivative of the pseudo control input used for the conventional case. A less invasive method to consider vehicle dynamics effect is by designing a model based reference model employed for the generation of the abovementioned derivative. With such method, the state dependent increment term, responsible for large deviations during agile maneuvering, is identified and removed for perfect tracking. In regard to the issue related to flight phase transitions, the concept of virtual control inputs (VCI) showed promising results in keeping the effectiveness of the actuators similar in different flight phases.

In addition to the knowledge available in the literature, further assessments conducted on it evidenced major limitations with regard to the methods identified. It is worth to mention that current methods used for state compensation do not provide a practical solution for real world systems. The extraction of the compensation term does not in fact consider states that are not directly part of the trajectory, but affect the state term equally, such as the angle of attack in the short period motion. There is also no model based compensation for external disturbances. Regarding differential flatness, it has been found that a flatness based compensation implemented in a conventional way leads to steady state errors when dealing with external disturbances.

The final goal of the work that follows the content of this report is to obtain real world evidence that a platform's disturbance rejection and trajectory tracking can be improved by enhancing the conventional

structure of an INDI controller with information about the actuators and dynamics.

Based on the findings, the improvements that will be implemented to reach this objective consist in a extension of the already mentioned higher order reference model so that it can use the feedback from the state to efficiently counteract disturbances and deal with model mismatch.

References

[1] Ronald van 't Veld, Erik-Jan Van Kampen, and Q Ping Chu. "Stability and Robustness Analysis and Improvements for Incremental Nonlinear Dynamic Inversion Control". In: *2018 AIAA Guidance, Navigation, and Control Conference*. DOI: 10.2514/6.2018-1127. eprint: https://arc.aiaa.org/doi/pdf/10.2514/6.2018-1127. URL: https://arc.aiaa.org/doi/abs/10.2514/6.2018-1127.

[2] B.J. Bacon, A.J. Ostroff, and S.M. Joshi. "Reconfigurable NDI controller using inertial sensor failure detection amp; isolation". In: *IEEE Transactions on Aerospace and Electronic Systems* 37.4 (2001), pp. 1373–1383. DOI: 10.1109/7.976972.

[3] Barton Bacon and Aaron Ostroff. "Reconfigurable flight control using nonlinear dynamic inversion with a special accelerometer implementation". In: *AIAA Guidance, Navigation, and Control Conference and Exhibit*. DOI: 10.2514/6.2000-4565. eprint: https://arc.aiaa.org/doi/pdf/10.2514/6.2000-4565. URL: https://arc.aiaa.org/doi/abs/10.2514/6.2000-4565.

[4] Pranav Bhardwaj, Stefan Raab, and Florian Holzapfel. "Higher Order Reference Model for Continuous Dynamic Inversion Control". In: Jan. 2021. DOI: 10.2514/6.2021-1130.

[5] Pranav Bhardwaj et al. "Integrated Reference Model for a Tilt-rotor Vertical Take-off and Landing Transition UAV". In: *2018 Applied Aerodynamics Conference*. DOI: 10.2514/6.2018-3479. eprint: https://arc.aiaa.org/doi/pdf/10.2514/6.2018-3479. URL: https://arc.aiaa.org/doi/abs/10.2514/6.2018-3479.

[6] Murat Bronz et al. "Development of A Fixed-Wing mini UAV with Transitioning Flight Capability". In: *35th AIAA Applied Aerodynamics Conference*. DOI: 10.2514/6.2017-3739. eprint: https://arc.aiaa.org/doi/pdf/10.2514/6.2017-3739. URL: https://arc.aiaa.org/doi/abs/10.2514/6.2017-3739.

[7] Abbas Chamseddine et al. "Flatness-based trajectory planning for a quadrotor Unmanned Aerial Vehicle test-bed considering actuator and system constraints". In: June 2012, pp. 920–925. ISBN: 978-1-4577-1095-7. DOI: 10.1109/ACC.2012.6315362.

[8] P. Cohn et al. "Commercial drones are here: The future of unmanned aerial systems". In: *Capital Projects & Infrastructure - McKinsey & Company* (Dec. 2017).

[9] Christophe De Wagter et al. "The NederDrone: A hybrid lift, hybrid energy hydrogen UAV". In: *International Journal of Hydrogen Energy* 46 (Mar. 2021). DOI: 10.1016/j.ijhydene.2021.02.053.

[10] Matthias Faessler, Antonio Franchi, and Davide Scaramuzza. "Differential Flatness of Quadrotor Dynamics Subject to Rotor Drag for Accurate Tracking of High-Speed Trajectories". In: *IEEE Robotics and Automation Letters* 3.2 (2018), pp. 620–626. DOI: 10.1109/LRA.2017.2776353.

[11] M. Fliess et al. "On Differentially Flat Nonlinear Systems". In: *IFAC Proceedings Volumes* 25.13 (1992). 2nd IFAC Symposium on Nonlinear Control Systems Design 1992, Bordeaux, France, 24-26 June, pp. 159–163. ISSN: 1474-6670. DOI: https://doi.org/10.1016/S1474-6670(17)52275-2. URL: https://www.sciencedirect.com/science/article/pii/S1474667017522752.

[12] Michel Fliess et al. "Flatness and defect of non-linear systems: introductory theory and examples". In: *International Journal of Control* 61 (June 1995), pp. 13–27. DOI: 10.1080/00207179508921959.

[13] Michel Fliess et al. "Sur les systèmes non linéaires différentiellement plats". In: 1992.

[14] A. Isidori. *Nonlinear Control Systems*. 3. Springer, London, 1995. DOI: 10.1007/978-1-84628-615-5.

[15] Xiang Li et al. “A Method to Compensate Interaction between Actuator Dynamics and Control Allocator under Incremental Nonlinear Dynamic Inversion Controller”. In: 428 (Oct. 2018), p. 012048. DOI: 10.1088/1757-899x/428/1/012048. URL: https://doi.org/10.1088/1757-899x/428/1/012048.

[16] Thomas Lombaerts and Gertjan Looye. “Design and flight testing of manual nonlinear flight control laws”. In: *AIAA Guidance, Navigation, and Control Conference*. DOI: 10.2514/6.2011-6469. eprint: https://arc.aiaa.org/doi/pdf/10.2514/6.2011-6469. URL: https://arc.aiaa.org/doi/abs/10.2514/6.2011-6469.

[17] Daniel Mellinger and Vijay Kumar. “Minimum snap trajectory generation and control for quadrotors”. In: *2011 IEEE International Conference on Robotics and Automation*. 2011, pp. 2520–2525. DOI: 10.1109/ICRA.2011.5980409.

[18] Luat T. Nguyen. “Simulator Study of Stall / Post Stall Characteristics of Fighter Airplane with Relaxed Longitudinal Stability”. In: *National Aeronautics and Space Administration, Scientific and Technical Information Branch* (1979).

[19] Michael W. Oppenheimer and David B. Doman. “Methods for Compensating for Control Allocator and Actuator Interactions”. In: *Journal of Guidance, Control, and Dynamics* 27.5 (2004), pp. 922–927. DOI: 10.2514/1.7004. eprint: https://doi.org/10.2514/1.7004. URL: https://doi.org/10.2514/1.7004.

[20] Florian Peter, Miguel Leitão, and Florian Holzapfel. “Adaptive Augmentation of a New Baseline Control Architecture for Tail-Controlled Missiles Using a Nonlinear Reference Model”. In: *AIAA Guidance, Navigation, and Control Conference*. DOI: 10.2514/6.2012-5037. eprint: https://arc.aiaa.org/doi/pdf/10.2514/6.2012-5037. URL: https://arc.aiaa.org/doi/abs/10.2514/6.2012-5037.

[21] Stefan A. Raab et al. “Consideration of Control Effector Dynamics and Saturations in an Extended INDI Approach”. In: *AIAA Aviation 2019 Forum*. DOI: 10.2514/6.2019-3267. eprint: https://arc.aiaa.org/doi/pdf/10.2514/6.2019-3267. URL: https://arc.aiaa.org/doi/abs/10.2514/6.2019-3267.

[22] Stefan A. Raab et al. “Proposal of a Unified Control Strategy for Vertical Take-off and Landing Transition Aircraft Configurations”. In: *2018 Applied Aerodynamics Conference*. DOI: 10.2514/6.2018-3478. eprint: https://arc.aiaa.org/doi/pdf/10.2514/6.2018-3478. URL: https://arc.aiaa.org/doi/abs/10.2514/6.2018-3478.

[23] Thomas Raffler, Jian Wang, and Florian Holzapfel. “Path Generation and Control for Unmanned Multirotor Vehicles Using Nonlinear Dynamic Inversion and Pseudo Control Hedging”. In: *IFAC Proceedings Volumes* 46.19 (2013). 19th IFAC Symposium on Automatic Control in Aerospace, pp. 194–199. ISSN: 1474-6670. DOI: https://doi.org/10.3182/20130902-5-DE-2040.00132. URL: https://www.sciencedirect.com/science/article/pii/S1474667015363217.

[24] Gerasimos G. Rigatos. *Nonlinear Control and Filtering Using Differential Flatness Approaches*. 1. Springer, Cham, 2015. DOI: 10.1007/978-3-319-16420-5.

[25] Richard Russell. “Non-linear F-16 Simulation using Simulink and Matlab”. In: (Aug. 2003).

[26] S. Sieberling, Q. P. Chu, and J. A. Mulder. “Robust Flight Control Using Incremental Nonlinear Dynamic Inversion and Angular Acceleration Prediction”. In: *Journal of Guidance, Control, and Dynamics* 33.6 (2010), pp. 1732–1742. DOI: 10.2514/1.49978. eprint: https://doi.org/10.2514/1.49978. URL: https://doi.org/10.2514/1.49978.

[27] P. Simplício et al. “An acceleration measurements-based approach for helicopter nonlinear flight control using Incremental Nonlinear Dynamic Inversion”. In: *Control Engineering Practice* 21.8 (2013), pp. 1065–1077. ISSN: 0967-0661. DOI: https://doi.org/10.1016/j.conengprac.2013.03.009. URL: https://www.sciencedirect.com/science/article/pii/S0967066113000634.

[28] Jean-Jacques E Slotine, Weiping Li, et al. *Applied nonlinear control*. Vol. 199. 1. Prentice hall Englewood Cliffs, NJ, 1991.

[29] Ewoud Smeur, Guido Croon, and Q. Chu. “Cascaded Incremental Nonlinear Dynamic Inversion Control for MAV Disturbance Rejection”. In: *Control Engineering Practice* 73C (Apr. 2018), pp. 79–90. DOI: 10.1016/j.conengprac.2018.01.003.

[30] Ewoud J. J. Smeur, Qiping Chu, and Guido C. H. E. de Croon. “Adaptive Incremental Nonlinear Dynamic Inversion for Attitude Control of Micro Air Vehicles”. In: *Journal of Guidance, Control, and Dynamics* 39.3 (2016), pp. 450–461. DOI: 10.2514/1.G001490. eprint: https://doi.org/10.2514/1.G001490. URL: https://doi.org/10.2514/1.G001490.

[31] Ezra Tal and Sertac Karaman. “Accurate Tracking of Aggressive Quadrotor Trajectories Using Incremental Nonlinear Dynamic Inversion and Differential Flatness”. In: *2018 IEEE Conference on Decision and Control (CDC)*. 2018, pp. 4282–4288. DOI: 10.1109/CDC.2018.8619621.

[32] Ezra A. Tal and Sertac Karaman. “Global Trajectory-tracking Control for a Tailsitter Flying Wing in Agile Uncoordinated Flight”. In: *AIAA AVIATION 2021 FORUM*. DOI: 10.2514/6.2021-3214. eprint: https://arc.aiaa.org/doi/pdf/10.2514/6.2021-3214. URL: https://arc.aiaa.org/doi/abs/10.2514/6.2021-3214.

A

MAVLab's Overactuated Quadplane

In this Literature Study report it has been mentioned, multiple times, how the bigger limitations to INDI controllers are mostly impactful for certain UAV designs and operations. To summarize, degradation in trajectory tracking arise when actuators are non-ideal and strong accelerations are required to follow the predefined trajectory (referred usually as agile maneuvering).

If, during the research following this study, a solution to counteract these limitations is found, it should be validated and tested on a platform that actually meets such characteristics. It is also important that such platform is available for real test flight, and not only simulations, because of the relevance of the topic in the practical field and the lack of outdoor test flight data on model based compensation solutions for INDI controllers.

In the past year, TUDelft's unmanned air vehicle laboratory, the MAVLab[1], designed and manufactured a new type of UAV: a dual-axis tilting rotor quad-plane, shown in Figure A.1. Choosing this platform to carry experiments and conduct test flights brings numerous advantages, listed below:

1. **Non Ideal Actuators**: the Quadplane tilting mechanism involves a wide set of servo actuators which act on the thrust direction. The combinations with gears makes the actuators of the vehicle not ideal. Based on what has been previously found, the neglection of their dynamics can affect negatively the overall flight performance.
2. **High Dependency on Wing Disturbances**: flying wing designs are notoriously bad in windy environments, due to their non-negligible wind surfaces. This is especially penalising in situations where low speed precision manoeuvres are required (such as precision landing in a gusty environment). However, the Quadplane special configuration allows for full 6 degrees of freedom control. This provides a good testing platform to validate the improved disturbance rejection capabilities of the new controller.
3. **Capability to Perform Aggressive Maneuvers**: the light design and the over-actuated setup allow the Quadplane to be capable to achieve agile maneuvering in all 6 degrees of freedom.
4. **Vehicle Already Manufactured and Flying on INDI Control**: the research around the Quadplane has been conducted now for over an year and still ongoing. To date, the vehicle is completely manufactured, the controller has been programmed and implemented successfully and, recently, manual flight were conducted on INDI control. This allows for the improved controller to be implemented on top of the existing INDI controller and tested without loosing time in tasks related to manufacturing and code base building.
5. **High Detail Simulator Running on INDI**: Together with the physical UAV and the code base, a high fidelity Matlab simulation environment is also available. This further simplifies the implementation of the newly developed controller in the over-actuated Quadplane case, allowing also for easier debugging and better understanding.

[1] https://mavlab.tudelft.nl/

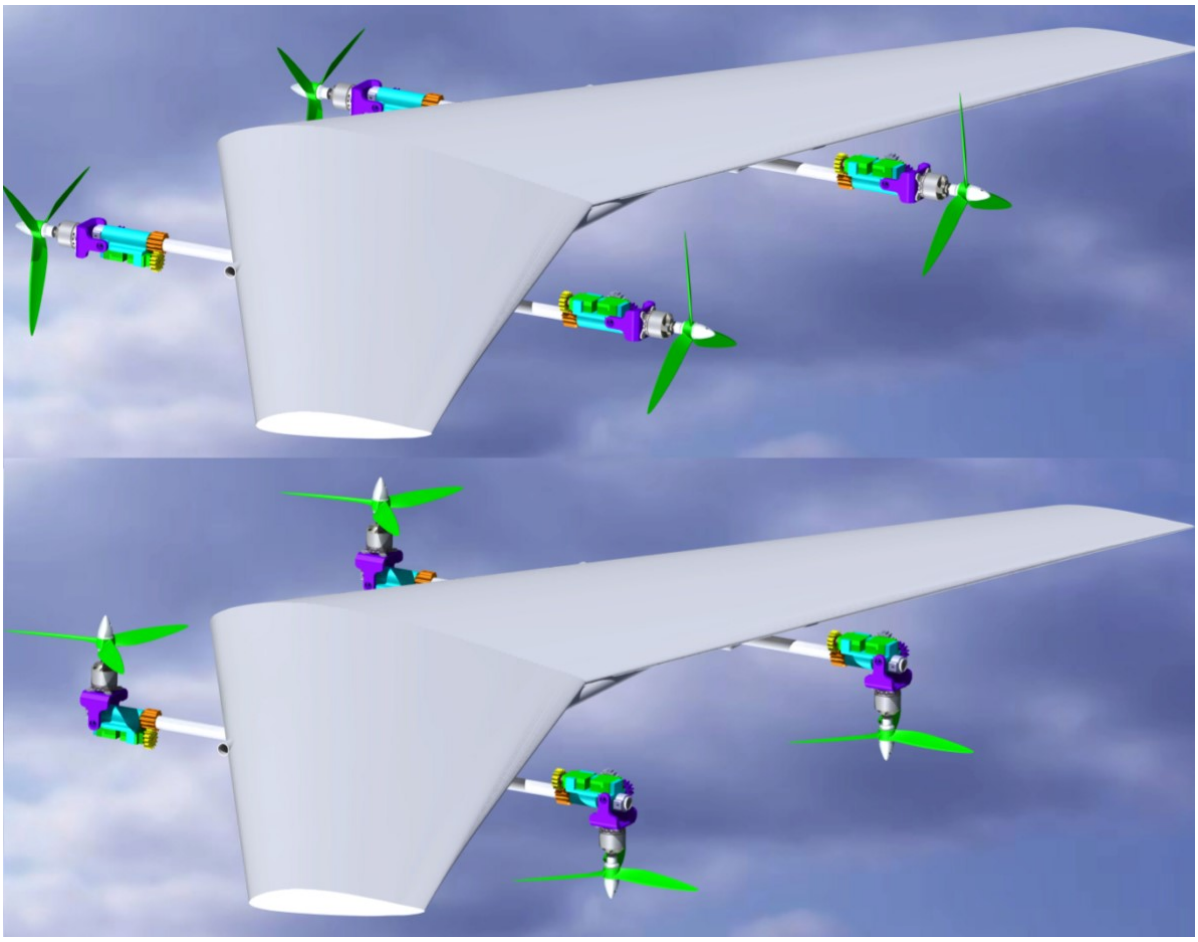

Figure A.1: Render of the experimental version of the over-actuated vehicle

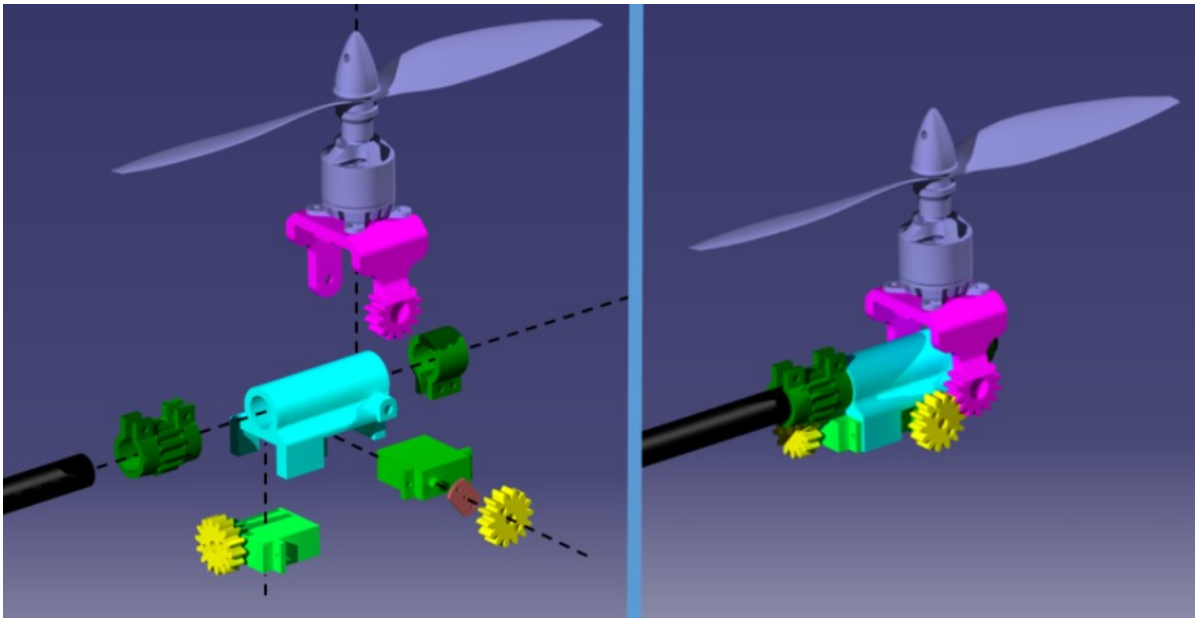

Figure A.2: Render of the tilting mechanism, exploded view on the right side and isometric view on the left side.